ChemComm

Dynamic Article Links

Cite this: *Chem. Commun.*, 2011, **47**, 9293–9311

www.rsc.org/chemcomm

FEATURE ARTICLE

Aqueous synthesis of CdTe nanocrystals: progresses and perspectives

Yilin Li, Lihong Jing, Ruirui Qiao and Mingyuan Gao*

Received 8th March 2011, Accepted 26th April 2011
DOI: 10.1039/c1cc11331c

As an alternative choice to CdSe nanocrystals synthesized in organic phase, CdTe nanocrystals synthesized in aqueous solution, have attracted increasing research interests in recent years. This feature article summarizes the aqueous solution-based syntheses, some optoelectronic applications, and bioapplications of CdTe nanocrystals, with emphasis on the recent progresses in related fields.

1. Introduction

II–VI semiconductor nanocrystals represent one of the most important types of nanomaterials. During the past three decades, the syntheses, physical properties of II–VI semiconductor nanocrystals, and their applications in various fields have received in-depth investigations.[1–10] Owing to the quantum confinement effect, II–VI semiconductor nanocrystals exhibit unique optical properties such as narrow, symmetric, and particle size-dependent fluorescence which is characterized by broad excitation ranges and excellent robustness against photobleaching.[2,4,5,8]

Up to now, the syntheses of II–VI semiconductor nanocrystals such as ZnS, ZnSe, CdS, CdSe and CdTe are achieved mainly through two synthetic routes. The first synthetic route, known as the TOP-TOPO method paved by Bawendi and co-workers in 1993,[3] relies on the pyrolysis of various types of precursors. In the earlier investigations, dimethylcadmium was used as a cadmium source and bis(trimethylsilyl)selenium or trioctylphosphine selenide was used as a Se source. In a non-polar high boiling point solvent, upon the pyrolysis of dimethylcadmium, and bis(trimethylsilyl)selenium or trioctylphosphine selenide, CdSe nanocrystals with well-defined optical properties were synthesized.[3] In spite of further improvements achieved by Peng and co-workers through replacing the hazardous dimethylcadmium by safer and greener precursors, such as cadmium oxide[11] or cadmium acetate,[12] there still exist inherent limitations in this synthetic route including high-cost, unfriendly and rigorous experimental conditions. Nevertheless, as the most mature products of this synthetic route, CdSe nanocrystals, including those with core/shell,[13,14] core/shell/shell,[14] and alloyed structures constructed in combination with other types of II–VI semconductors,[15] have represented the most successful examples of fluorescent nanocrystals and become almost the symbol of fluorescent semiconductor nanocrystals as well.

The second main synthetic route for II–VI semiconductor nanocrystals relies on simple precipitation reactions taking place in aqueous systems containing various types of surface capping ligands. This aqueous synthetic route was established earlier[1,16] and become mature in the 1990s.[17–23] During that period of time, CdS nanocrystals were one of the most

Institute of Chemistry, the Chinese Academy of Sciences, Bei Yi Jie 2, Zhong Guan Cun, Beijing 100190, China. E-mail: gaomy@iccas.ac.cn; Fax: +86 10 8261 3214

Yilin Li

Yilin Li received her Master's Degree in Pharmaceutical Analysis from the Beijing Institute of Pharmacology and Toxicology in 2008. Since then, she has been a PhD candidate under the supervision of Prof. Dr Mingyuan Gao in the Institute of Chemistry, the Chinese Academy of Sciences. Her major research interests are the applications of semiconductor nanocrystals in cell imaging and cancer detection.

Lihong Jing

Lihong Jing currently is a PhD candidate of successive postgraduate and doctoral degrees under the supervision of Prof. Dr Mingyuan Gao in the Institute of Chemistry, the Chinese Academy of Sciences. Her major research focuses on the synthesis and biological applications of inorganic fluorescent semiconductor nanocrystals and nanocrystal-based functional composite nanomaterials.

successful products of this synthetic route and widely used as a model for understanding different phenomena related to semiconductor nanocrystals.[1,16–18] However, the emergence of the TOP-TOPO method largely shifted the research interests of the community of nanoparticle synthesis from CdS nanocrystals synthesized in aqueous system to CdSe nanocrystals synthesized in organic phase by the TOP-TOPO method. Owing to a suitable bandgap, CdSe nanocrystals exhibit the most remarkable particle size-dependent fluorescence covering the whole visible light range.[14,24] An important breakthrough for the aqueous synthetic route however was achieved by Gao *et al.* in 1998 in synthesizing highly fluorescent CdTe nanocrystals in aqueous systems by choosing mercapto acids as stabilizing agent,[23] on the basis of earlier works of Henglein,[2] Weller and Rogach.[21,22] Since CdTe has a slightly narrower bandgap than CdSe,[13] the fluorescence of CdTe nanocrystals can be tuned from the bluish green to near infrared range *via* careful control over the particle size.[25,26] Consequently, CdTe nanocrystals as the representative of semiconductor nanocrystals directly synthesized in aqueous solutions has become an alternative choice of fluorescent semiconductor nanocrystals for many investigations. Nevertheless, it remains challenging to apply the aqueous synthetic approach to delicate surface engineering, *i.e.*, constructing shells of other types of semiconductors for fine tuning the optical properties of the resultant nanocrystals, as the TOP-TOPO method does for CdSe nanocrystals.[13,14] This is because water is a strong polar solvent and it readily induces heavy surface dynamics which gives rise to extra difficulties in constructing nanocrystals with complex structures. Nevertheless, in comparison with the TOP-TOPO method, the aqueous synthetic route is characterized by relatively simpler, cheaper and less toxic processes.

With respect to applications, CdTe nanocrystals are rather comparable to CdSe nanocrystals. They both can be used as light-emitting materials in optoelectronic devices,[27] cell labeling,[9,10,28] and *in vivo* bioimaging.[9,10,29,30] However, for optoelectronic applications, the processing of water-soluble nanocrystals is undoubtedly more environmentally friendly than the organic soluble nanocrystals. For biomedical applications, the extendability of the photo-emission into the near infrared region makes CdTe nanocrystals more suitable for biomedical investigations, although the bio-safety of cadmium calcogenides as a whole remains under vigorous debates.

In this feature article, we summarize the aqueous solution-based syntheses, optoelectronic applications and bioapplications of CdTe nanocrystals, and meanwhile highlight our recent research activities in highly fluorescent CdTe nanocrystals, CdTe nanocrystal-based composite nanoparticles and microspheres, cancer cell labeling, and visualization of cancer cell apoptosis using CdTe nanocrystal-based fluorescent bioprobes. In addition, some low-dimensional CdTe nanomaterials as extensions of the zero-dimensional CdTe nanocrystals will also be briefly mentioned.

2. Aqueous synthesis of CdTe nanocrystals

The earliest successful example on the aqueous synthesis of CdTe nanocrystals was obtained *via* a precipitation reaction between Cd^{2+} and Na_2Te in the presence of polyphosphate with a formula of $(NaPO_3)_6$ as stabilizing agent,[2] which apparently inherited the well-established recipe for fluorescent CdS nanocrystals synthesized directly in aqueous solution except that Na_2Te was used instead of Na_2S or H_2S.[2] The resultant CdTe nanoparticles do not show fluorescence. However, upon illumination or attack by free radicals generated radiolytically they acquire fluorescence.[2] Although much deeper understanding on these phenomena was arrived at later on,[31–36] the great contribution of this investigation on the aqueous synthesis of CdTe nanocrystals should not fade with time.

An important breakthrough for synthesizing long-term stable fluorescent CdTe nanocrystals was achieved by Rogach *et al. via* the use of thioglycerol and mercaptoethanol as surface stabilizing agent.[22] Since thiol molecules can firmly stick to the surface of the resultant nanocrystals *via* Cd–SR

Ruirui Qiao

Ruirui Qiao received her Master Degree in Medicinal Chemistry in 2007 from the School of Pharmaceutical Science, Peking University. After that, she has been working with Prof. Mingyuan Gao in the Institute of Chemistry, the Chinese Academy of Sciences, as a research assistant. Her major research interests are development and application of nanocrystal-based molecular imaging probes for cancer detections.

Mingyuan Gao

Dr Mingyuan Gao is currently a full Professor in the Institute of Chemistry, the Chinese Academy of Sciences. His main research interests include: synthesis of nanocrystals with novel properties, unusual shapes, and structures; synthesis of organic/inorganic hybrid materials; biological, biomedical, and environmental applications of functional nanomaterials. He took his current position upon the 'Hundred-talent Program' from CAS. He received the 'National Science Fund for Distinguished Young Scholars' from NSFC in 2002. He was an AvH fellow between 1996 and 1998. So far, he has published ~90 peer-reviewed articles and holds 13 patents. More details can be found at http://www.gaomingyuan.com.

bonds, they can effectively prevent the nuclei from uncontrollable growth. Although under optimized conditions, the exciton emission can be achieved from CdTe nanocrystals stabilized by thioglycerol or mercaptoethanol, the fluorescence efficiency remains lower than 3%.[22] Nevertheless, these early investigations opened the door to intensive investigations on the aqueous synthesis of CdTe nanocrystals.

2.1 The remarkable role of mercapto acids in highly fluorescent CdTe nanocrystals

The synthesis of CdTe nanocrystals capped by various types of thiol molecules has comprehensively been summarized in a number of review articles.[25,26,28] It has been demonstrated that the optical properties of the as-prepared CdTe nanocrystals are strongly dependent on the nature of the thiol molecules serving as stabilizing agents, among them mercapto acids such as thioglycolic acid (TGA) and mercaptopropionic acid (MPA) are the most important ones for achieving highly fluorescent CdTe nanocrystals.

The first successful example of TGA as stabilizing agent for CdTe nanocrystals was reported by Gao and co-workers.[23] The resultant CdTe nanocrystals only present a fluorescence efficiency of a few percent. However, the fluorescence intensity of the as-prepared CdTe nanocrystals can be greatly enhanced by lowering the pH of the mother-solution with a maximum fluorescence efficiency reaching 18% at pH 4.5 as shown in Fig. 1. Even though TGA was previously used to stabilize CdS nanoparticles,[37] it was not noticed that it can be so important for obtaining highly fluorescent CdTe nanocrystals. Systematic investigations suggest that in acidic range, the thioglycolic acid and cadmium ion excess in the mother-solution will deposit on the surface of CdTe nanocrystals forming a shell layer structure comprised of Cd-TGA complexes due to the secondary coordination between the carbonyl group of TGA and the primary thiol-coordinating cadmium.[38,39] As the Cd-TGA complexes can effectively eliminate the non-radiative pathway for excitons, analogous to the CdS or ZnS shell for highly fluorescent CdSe nanocrystals, the fluorescence efficiency is greatly increased.

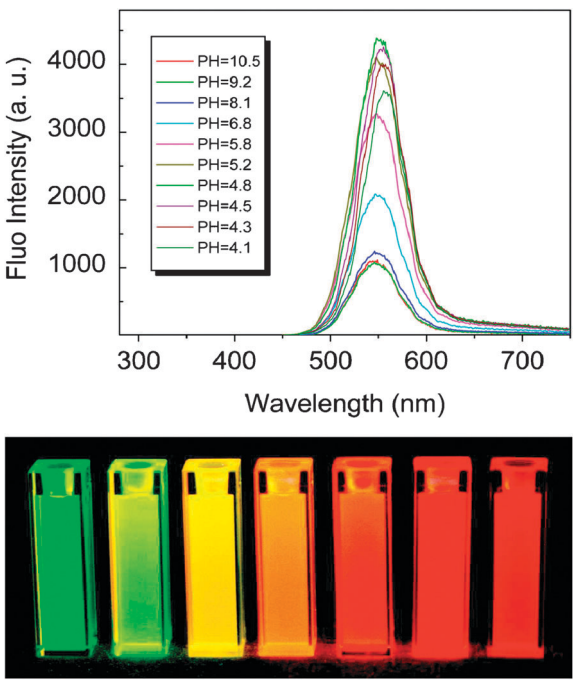

Fig. 1 Upper panel shows the pH-dependent fluorescence behavior recorded from an aqueous solution of freshly prepared TGA-capped CdTe nanocrystals during the titration process by using 0.1 M HCl (reprinted from ref. 23). Lower panel presents a photograph of aqueous solutions of seven differently sized CdTe nanocrystals after their fluorescence being optimized by pH. This photograph was taken by Gao between late 1997 and early 1998 in the lab of Prof. Horst Weller.

Similar pH-dependent fluorescence was also observed from following investigations of Zhang, Yang, Gao and co-workers on the MPA-capped CdTe nanocrystals.[40] However, the fluorescence intensity reaches its maximum at pH 6.0 rather than pH 4.5 for TGA-stabilized CdTe nanocrystals. The main difference between TGA and MPA in chemistry is pK_{COOH}, *i.e.*, 3.53 for TGA and 4.32 for MPA. The pH value for partly protonating the carboxylic group of MPA is consequently higher than that for TGA. By using poly(acrylic acid) as a model compound, it was further revealed that the carboxyl oxygen of the protonated carboxylic group can effectively coordinate with the cadmium ion on the surface of CdTe nanocrystal at lower pH, which partly contributes to the fluorescence enhancement effect. Meanwhile, such coordination also helps the excess MPA molecules to deposit on the surface of the resultant nanocrystals to form a shell of Cd-MPA complexes by combining with excess cadmium ions in the solution, which can effectively give rise to enhanced fluorescence.[40]

Apart from TGA and MPA, glutathione as mercapto acid derivative was also used for achieving CdTe nanocrystals with fluorescence efficiency higher than 50%.[41,42] Some reports attribute the high fluorescence efficiency to the formation of CdTe@ZnS core/shell[43] or $Cd_xZn_{1-x}Te$ alloy structures[44] as glutathione is likely to be more prone to thermal decomposition than other thiol ligands.[41,42] Very recently, it was shown that the protein ribonuclease A can be used as stabilizer for synthesizing CdTe nanocrystals with fluorescence higher than 70%.[45] However, it remains unclear why ribonuclease A is so effective for achieving highly fluorescent CdTe nanocrystals due to the complexity of the interactions between proteins and semiconductor nanocrystals in general.

Although 2-mercaptoethylamine or 2-(dimethylamino)-ethanethiol were also used for stabilizing CdTe nanocrystals with relatively high fluorescence efficiency, the resultant nanocrystals only present moderate colloidal stability in aqueous solutions.[26] In contrast, the fluorescence efficiency of the as-prepared TGA- and MPA-capped CdTe nanocrystals can reach 40–60% after further optimizing the synthetic parameters such as thiol/Cd ratio, pH value, Te/Cd ratio, precursor concentration, *etc.*[25,46,47] In addition, the TGA- and MPA-stabilized CdTe nanocrystals present excellent colloidal stability of years. Most importantly, the later works on the low-dimensional CdTe nanorods,[48] nanowires,[49] nanotubes,[39] and twisted ribbons[50] are also strongly associated with the use of mercapto acids as stabilizing agents.

2.2 Core/shell structures for achieving highly fluorescent CdTe nanocrystals

Epitaxially growing wide bandgap inorganic semiconducting materials on the surface of fluorescent nanocrystal core with narrower band-gap has been demonstrated to be an effective approach for effectively eliminating the surface traps of the core nanocrystals and so lead to high fluorescence efficiency. A number of successful examples on CdSe nanocrystals with either ZnS or CdS shells have been reported based on the TOP-TOPO synthetic route.[13,14] Nevertheless, by the conventional aqueous synthetic route as described above, it is rather difficult to construct such core/shell structures due to the fact that water is such a strong polar solvent that it can not only coordinate with cadmium ions in different forms depending on the pH of the system, but also readily induce complicated dynamics for surface capping molecules.

Our group firstly reported the preparation of CdTe@CdS core/shell nanocrystals with fluorescent efficiency around 85%, as shown in Fig. 2, *via* an illumination-assisting process.[31] As a matter of fact, it was observed that the TGA-stabilized CdTe nanocrystals presented a fluorescence enhancement effect upon aging under ambient conditions more than 10 years ago. More systematic studies revealed that the UV component in ambient light readily induce the degradation of TGA even in a strictly controlled oxygen-free environment in the alkaline range. Upon illumination of ambient light, TGA is degraded to firstly form dithioglycolic acid. In alkaline range, dithioglycolate is further degraded *via* very complicated chemical processes, forming thioglyoxylate which can slowly release sulfide ions upon further decomposition, as illustrated in Scheme 1.[31] Upon systematic investigations by combining conventional absorption spectroscopy, fluorescence spectroscopy, X-ray diffractometry, with careful analysis of X-ray photoelectron spectroscopy results on CdTe nanocrystals obtained at different aging stages, it is revealed that the slowly released sulfide ion will deposit on the surface of CdTe nanocrystals in combination with cadmium ions, forming a CdTe@CdS core/shell structure which can greatly increase the fluorescence efficiency of the resultant nanocrystals.[31] These investigations clearly reveal the fluorescence enhancement effects caused by aging the TGA-stabilized CdTe nanocrystals under ambient conditions, though the whole process remains too time-consuming for preparing CdTe@CdS core/shell structured nanocrystals with extremely high fluorescence efficiency. Nevertheless, these investigations suggest that by properly controlling the growth kinetics of the shell material, it remains possible to form a broader bandgap shell on a CdTe core *via* the aqueous synthetic route for further increasing the fluorescence efficiency of the CdTe nanocrystals.

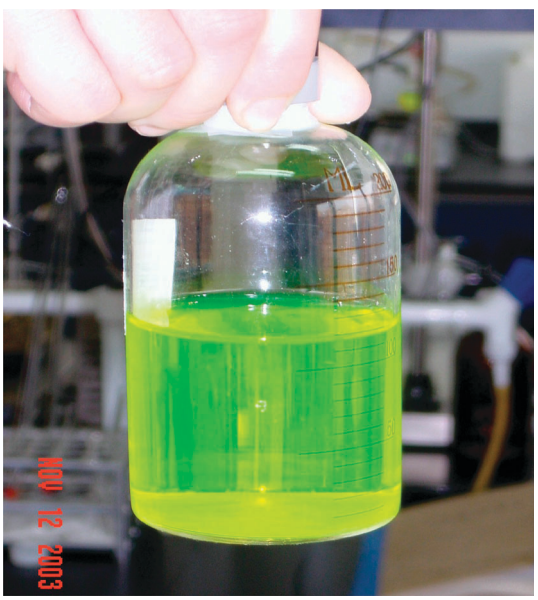

Fig. 2 Photograph of an aqueous solution of CdTe@CdS core/shell nanocrystals with fluorescence efficiency up to 85%. This photograph was taken under ambient conditions in the absence of additional excitation light. The shining yellow–green color is from the fluorescence of the nanocrystals (reprinted from ref. 31).

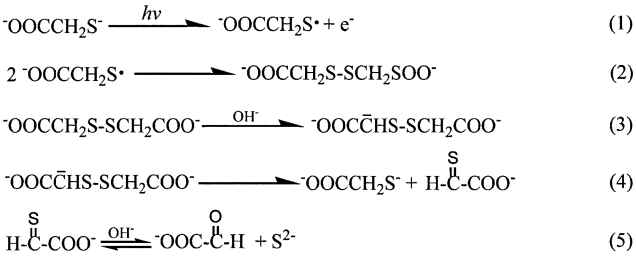

Scheme 1 Overall reactions initiated by illumination for TGA in alkaline solution (reprinted from ref. 31).

Following on from these early investigations, thermally unstable sulfide compounds such as thioacetamide,[51] thiourea,[52] or glutathione[53] are also successfully used instead of TGA for slowly releasing sulfide ions in coating CdTe nanocrystals with a CdS shell. Recently, it is demonstrated that the growth of CdS shell on CdTe core in aqueous solution can also be achieved in a more efficient way with the aid of microwave irradiation instead of illumination. For example, CdTe@CdS core/shell nanocrystals with fluorescence efficiency up to 75% were achieved by microwave irradiation within 5 min at 100 °C in coating MPA-stabilized CdTe nanocrystals suspended in a solution containing $CdCl_2$, Na_2S and MPA.[54] The emission peak position of the resultant nanocrystals can be tuned in a range of 535–623 nm.[54] Alternatively, CdTe@CdS core/shell nanoparticles were also obtained with the aid of ultrasonic irradiation from a system containing cadmium acetate, thiourea and as-prepared thioglycerol-capped CdTe nanocrystals.[55]

Although these successful progresses have made the synthesis of CdTe-based core/shell nanocrystals *via* the aqueous synthetic route more feasible, the control over the thickness of the CdS shell remains challenging. Very recently, successive ion layer adsorption and reaction, which was developed by Peng in preparing CdSe@CdS nanocrystals in the organic phase,[56] was adopted to synthesize CdTe@CdS nanocrystals in aqueous system.[57] In this study, calculated amounts of Cd and S ions were injected at a certain speed into the solutions containing pre-purified MPA-capped CdTe nanocrystals. The thickness of the CdS shell was controlled by the stoichiometry of the injection solutions. By coating three layers of CdS, the

fluorescence efficiency of CdTe nanocrystals was significantly increased by a factor of 5, reaching 40%. Furthermore, the author claimed that the CdTe@CdS nanocrystals can evolve from type I to type II structure with increasing amount of CdS.[57]

So far, the syntheses of CdTe@CdS core/shell nanocrystals as mentioned above all contain two successive steps, *i.e.* preparation of CdTe cores followed by subsequent growth of the CdS shell. Recently, Choi and co-workers developed a one-pot synthetic route for achieving CdTe@CdS core/shell nanocrystals with near-infrared fluorescence by a hydrothermal method.[58] $CdCl_2$ and NaHTe and *N*-acetyl-L-cysteine (NAC) were chosen as starting materials. NAC was used not only as stabilizing agent, but also as a source of sulfide ion for the CdS shell growth. Upon reaction at 200 °C in a steel autoclave, CdTe@CdS core/shell nanocrystals with maximal fluorescence efficiency of 62% were obtained and the emission peak was tuned in a range of 650–800 nm.[58]

In addition to CdTe@CdS, CdTe@CdSe,[59] CdTe@ZnTe,[60] and CdTe@ZnS[43] core/shell, and CdTe@CdS@ZnS core/shell/shell nanocrystals[61,62] are recently reported based on the classic aqueous synthetic route or with the aid of microwave irradiation upon introducing suitable shell precursors into the colloidal solution of CdTe nanocrystals. In general, the constructions of these core/shell structures are demonstrated to be effective for increasing the fluorescence efficiency of CdTe core. For example, the room-temperature fluorescence efficiency of CdTe@ZnS nanocrystals reaches 84%,[43] while that of CdTe@CdS@ZnS nanocrystals obtained by microwave synthesis is around 80%.[62] Most importantly, the release of Cd^{2+} from the CdTe core can greatly be suppressed,[43,62] which is good news for providing CdTe nanocrystal-based fluorescent probes for bio-related applications.

In fact, achieving core/shell structured nanocrystals in aqueous systems remains highly challenging. Due to the small difference of electron density between CdTe and II–VI semiconductor shells, it is difficult to identify the core/shell structures mentioned above by conventional transmission electron microscopy. Therefore, more experimental proofs may be required to support the statements made for some of the aforementioned core/shell structures.

2.3 CdTe-based alloyed nanocrystals

The mercapto acid-based aqueous synthesis of CdTe nanocrystals was further exemplified in anionic alloyed semiconductor nanocrystals. Kotov and co-workers reported that a spontaneous transition of L-cysteine-stabilized CdTe nanocystals to CdTeS alloyed nanocrystals and then to CdS nanocrystals can be induced by ethylenediaminetetraacetic acid (EDTA) dipotassium salt dehydrate which acts as a catalyst for partially removing thiol stabilizers from the nanoparticle surface.[63] Such structural transitions were followed and confirmed by absorption and luminescence spectroscopy results on samples extracted at different stages. In this process, EDTA can facilitate the release of Te^{2-}, while the following oxidation of Te^{2-} drives the compositional transition of CdTe towards CdS *via* CdTeS without an additional S source except for L-cysteine. As the whole process is relatively slow, the alloyed nanocrystals with various compositions are allowed by manipulating the transition process upon addition or removal of EDTA.

By a different strategy, Rogach and co-workers reported $CdSe_xTe_{1-x}$ alloyed nanocrystals prepared by simultaneous reactions of NaHSe and NaHTe with Cd^{2+} in the presence of TGA.[64] By varying the ratio of NaHSe to NaHTe and the refluxing time, the absorption onset of the resultant $CdSe_xTe_{1-x}$ nanocrystals were tuned over a wavelength region of 550–690 nm.[64]

In a similar way, CdTe-based cationic alloyed nanocrystals can also be prepared using the classic aqueous synthetic route, by simultaneously introducing different types of cationic ions into the reaction system, TGA- and MPA-capped $Cd_xHg_{1-x}Te$ nanocrystals were investigated by Ren,[65] Wang,[66] and Eychmüller,[67] respectively. By varying the Cd to Hg ratio, the fluorescence was successfully tuned from red to the near-infrared spectral region, which makes the resultant $Cd_xHg_{1-x}Te$ nanocrystals attractive candidates as amplifier media in telecommunication or as fluorescent probes for *in vivo* imaging studies.[67] A similar route was also adopted in synthesizing $Cd_xZn_{1-x}Te$ nanocrystals with fluorescence efficiency up to 75%.[44]

In comparison with the single component semiconductor nanocrystals, the energetic levels of conduction and valence bands of alloyed semiconductor nanocrystals can precisely be tuned by varying the degree of alloying, which thus opens up additional options for engineering nanocrystals with different electronic and optical properties.[64]

2.4 Other developments on CdTe nanocrystals

Apart from being important for fluorescence efficiency, Tang and co-workers recently found that the chirality of stabilizers such as L-cysteine and D-cysteine can also introduce chiral sites to the surface of the CdTe nanocrystals synthesized in aqueous solution,[68] which may open up a promising avenue for synthesizing CdTe nanocrystals with optical activities.

As extensions of the conventional aqueous synthetic route, the hydrothermal[69] and microwave-assisted synthesis[70–72] of CdTe nanocrystals in aqueous solution had been demonstrated. Although both of these two methods can effectively accelerate the growth of the CdTe nanocrystals, the microwave-assisted synthesis is more feasible for controlling the optical properties of the resultant nanocrystals. For example, TGA-capped CdTe nanocrystals with fluorescence efficiency of 82% can be obtained within 15 min under microwave irradiation,[70] while MPA-capped CdTe nanocrystals with emission in near-infrared region (733 nm) can be obtained within 45 min.[72]

3. Synthesis of CdTe nanocrystal-based fluorescence nanomaterials

It is so far well-accepted that the fluorescence of II–VI nanocrystals is intrinsically related to the surface traps. Although significant progresses have been achieved in synthesizing highly fluorescent CdTe nanocrystals by choosing appropriate surface capping agents or constructing suitable core/shell type structure, it remains fundamentally very

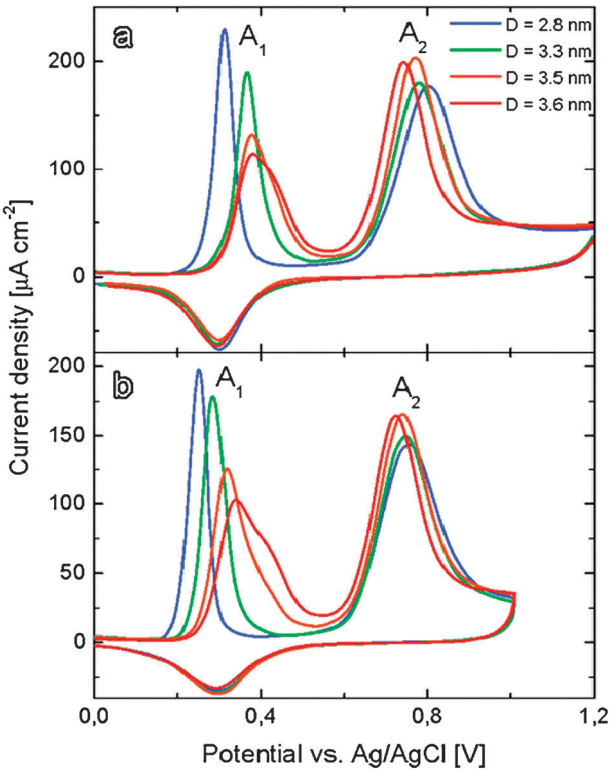

Fig. 3 Voltammograms recorded using Au electrode immersed in buffer solutions of TGA-capped CdTe nanocrystals of four different sizes (a) or in blank buffer solution after preadsorption of the same nanocrystals on the Au electrodes (b). The potential sweep rate was 20 mV s^{-1} (reprinted from ref. 74).

important to understand the chemical nature of the surface traps. As nanocrystals are rich in surface dangling bonds, suitable surface chemical structures are necessary to saturate the dangling bonds so as to increase the fluorescence efficiency.

Previous studies have demonstrated that Cd-related surface traps will lead to red-shifted fluorescence with greatly reduced fluorescence efficiency.[73] Nevertheless, the Te-related surface traps cannot so simply be detected by optical spectroscopy. In 2000, we started to use electrochemical methods to study Te-related surface traps in TGA- and MPA-capped CdTe nanocrystals. It was found out that there exist several distinct oxidation and reduction peaks in the voltammograms of TGA-capped CdTe nanocrystals as shown in Fig. 3.[74] The oxidation peak between 0.75 and 0.8 V (Peak A_2) shows a clear nanocrystal-size dependent behavior, which can be explained by the shifting of energetic band positions caused by the quantum size effect. However, the anodic peak located between 0.3 and 0.4 V (Peak A_1) shows an extraordinary nanocrystal-size dependent behavior. Systematic studies revealed that the oxidation peak A_1 can be assigned to Te-related trap states. It was further confirmed that the contribution of the charge associated with this peak compared to the total charge passed during the oxidation of CdTe nanocrystals correlates well with the fluorescence efficiency.[74]

Apart from the strong surface-dependent fluorescence, the release of toxic Cd^{2+} upon photooxidation, and the chemical and colloidal instabilities of CdTe nanocrystals in harsh environments remain obstacles for further extending their applications, especially to bioimmunoassays. In this context, encapsulating CdTe nanocrystals by inert materials are expected to be an effective measure for impeding the leakage of heavy metal ions into the environment, and meanwhile preventing the nanocrystals from being oxidized by ambient oxygen for suppressing the generation of surface defects. Moreover, simultaneous integration of differently sized CdTe nanocrystals in a microsphere also provides a facile approach for producing versatile fluorescent probes useful for high-throughput detections.[75,76]

3.1 Fluorescent SiO_2 particles incorporated with CdTe nanocrystals

By using the well-known Stöber method, Liz-Marzán and co-workers succeeded in coating aqueous CdS nanocrystals stabilized by sodium citrate and obtained core/shell type composite particles. They also demonstrated that the silica shell can suppress the photochemical oxidation of the encapsulated CdS nanocrystals.[77] The Stöber method is used for coating organic-soluble nanocrystals with silica,[77–86] the diameter of the final silica particles can be tuned from tens of nanometre to micrometres by means of seeded growth.[84] Apart from the Stöber approach, the reverse microemulsion approach can also be used for coating aqueous II–VI nanocrystals with silica upon hydrolysis of silica precursors in the microwater pool. The great advantage of the latter method is that it can yield more uniform silica spheres in the size range of 30–150 nm.[78] Nevertheless, both of these two approaches face the same difficulties, *i.e.*, how to maintain the fluorescence of the encapsulated nanocrystals and control the composite structures.[86]

Recently, important breakthroughs in synthesizing highly fluorescent silica particles with controllable composite structures have been achieved by our group using the reverse microemulsion method.[87–89] A microemulsion system comprised of cyclohexane, Triton X-100 (*t*-octylphenoxypolyethoxyethanol), *n*-hexanol, ammonia and CdTe nanocrystals co-stabilized by TGA and 1-thioglycerol (TGOL) was prepared and then TEOS (tetraethyl orthosilicate) as silica precursor was introduced. Upon hydrolysis and the following condensation of TEOS in water-in-oil emulsions, silica-coated CdTe nanocrystals were obtained.[87] By this approach, uniform CdTe@silica particles of 45–109 nm were obtained.[88] Our earlier investigations demonstrated that CdTe@silica particles with fluorescence efficiency up to 7% can be obtained, though this value is lower than that of the original CdTe nanocrystals. Quite unexpectedly, the resultant composite particles show a very unique core/shell structure, *i.e.*, each composite particle containing only one CdTe nanocrystal as core as shown in Fig. 4, which was demonstrated to be independent of the amount of CdTe nanocrystals.[87]

The formation mechanism for such CdTe@SiO_2 core/shell structures can be understood as follows. In the reverse microemulsion system mentioned above, cyclohexane serves as a continue phase, and Triton X-100 and *n*-hexanol are used as surfactant and co-surfactant, respectively. The aqueous solution of CdTe nanocrystals and ammonia is emulsified

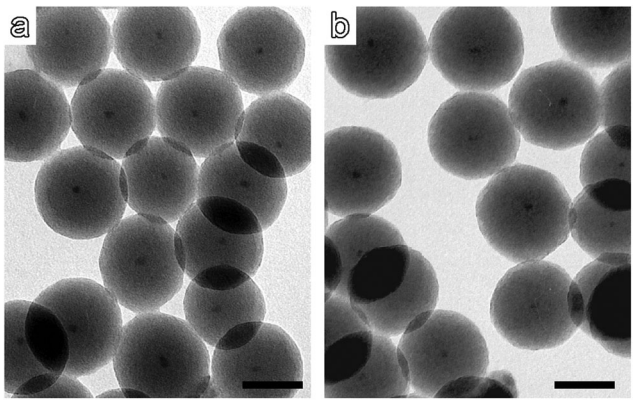

Fig. 4 TEM images of core/shell-structured CdTe@SiO_2 particles prepared under different initial concentrations of CdTe nanocrystals: (a) 1.35×10^{-5} M; (b) 5.40×10^{-6} M (with respect to CdTe nanocrystals). The scale bars correspond to 50 nm (reprinted from ref. 87).

under stirring forming micro water droplets. During this stage, the electrostatic repulsion between the negatively charged CdTe nanocrystals is effectively screened by the positive background arising from cations, *i.e.*, NH_4^+ and Na^+. In other words, the system is under an electrostatic equilibrium, which is supported by the fact that the aqueous solution of CdTe nanocrystals shows long term colloidal stability (over years) at pH 11. The average distance between CdTe nanocrystals initially should be larger than the Debye screening length D, as described by Debye–Hückel theory, so that the electrostatic equilibrium can be preserved. After the introduction of TEOS, which can dissolve well in cyclohexane, TEOS will pass through the oil/water interface by diffusion and start to hydrolyze upon the catalysis of ammonia. The partly hydrolyzed TEOS molecules have strong hydrophilicity due to the deprotonation of the silanol groups.[90–92] When these hydrolyzed species gain enough hydrophilicity, they will completely enter the aqueous phase. The subsequent condensation between hydrolyzed species in reverse micelles results in silica oligomers or silica intermediates which can be taken as a negatively charged polyelectrolyte as the pK_a of the silanol groups is around 7.[88] Thereafter, the previously established electrostatic equilibrium is destroyed. As the molecular weight of the oligomeric silica intermediates increases, the region around the oligomeric intermediates becomes locally negatively charged as the induced cations are evenly distributed throughout the microscale water pool. This local negatively charged background will reduce the screening between CdTe nanocrystals. Consequently, the Debye screening length for CdTe nanocrystals will increase, which introduces a net repulsion between two neighboring CdTe nanocrystals. As the sol–gel process proceeds, especially when the Debye screening length becomes larger than the radius of the microwater pool, most of the semiconductor nanocrystals will be driven to the boundary of the aqueous microdroplet, except for the last CdTe nanocrystals located at the center of the water pool due to the symmetry of the repulsive interaction between this specific CdTe nanocrystal and the others within the microwater pool.[87,88]

According to this mechanism, poly(diallyldimethylammonium chloride) (PDDA) was introduced into the microemulsion system to balance the electrostatic interactions between the silica intermediates and the CdTe nanocrystals, and the number of CdTe nanocrystals incorporated in each silica particle were found to be well correlated to the amount of PDDA.[87]

Very recently, we further demonstrated that by incubating TGA-stabilized CdTe nanocrystals in ammonia solution, the surface charge density of CdTe nanocrystals can be reduced, which also leads to multicore/shell CdTe@SiO_2 particles.[89] Most importantly, the pre-incubation process gives rise to high fluorescence retention due to the CdTe@CdS core/shell structure formed during the incubation process. Under optimized conditions, the fluorescence efficiency of the final composite particles as shown in Fig. 5 reaches 47% at room temperature.[89]

3.2 Fluorescent polymer beads incorporated with CdTe nanocrystals

Apart from silica, organic polymers as alternative choices are widely used for coating inorganic nanocrystals in forming semiconductor nanocrystal-based fluorescent nanomaterials. In general, the incorporation of semiconductor nanocrystals into polymers can be implemented upon two strategies: (1) physically confining semiconductor nanocrystals into porous polymer matrices *via* electrostatic, hydrogen-bonding or hydrophobic interactions; (2) polymerizing radical monomers in the presence of semiconductor nanocrystals.[93]

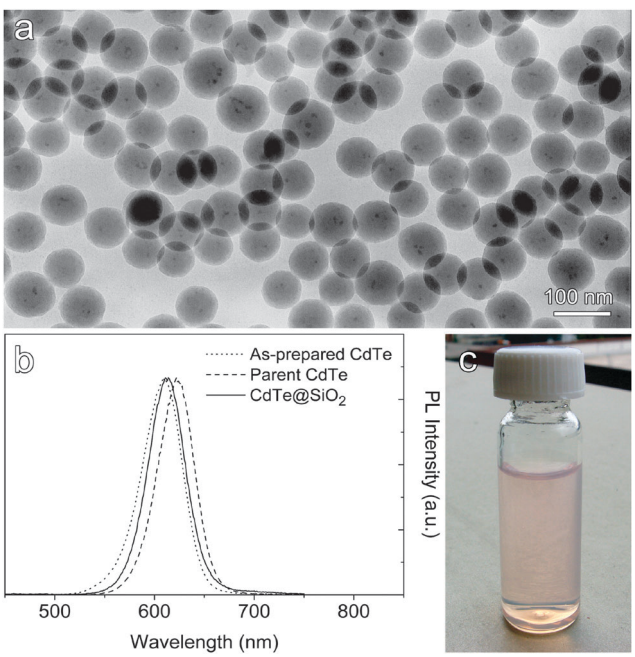

Fig. 5 (a) Representative TEM image of CdTe@SiO_2 particles prepared using CdTe nanocrystals which have been incubated for 8 days in ammonia solution. (b) Normalized fluorescence spectra of the as-prepared CdTe nanocrystals, incubated CdTe nanocrystals, and the CdTe@SiO_2 particles shown in (a). (c) Photograph of an aqueous dispersion of CdTe@SiO_2 particles taken under ambient conditions (reprinted from ref. 89).

Following the first strategy, we chose pNIPAM-based copolymers (pNIPAM = poly(*N*-isopropylacrylamide)) as matrices for encapsulating aqueous CdTe nanocrystals for forming fluorescent polymeric beads.[94,95] Through self-cross-linking effect, pNIPAM in water can form hydrogel spheres which will undergo a volume phase transition upon the variation of environment temperature or in the presence of external stimuli.[95] Utilizing these unique features, Wang, Gao and co-workers have demonstrated that fluorescent polymer spheres can be obtained by loading TGA-capped CdTe nanocrystals within *N*-isopropylacrylamide and 4-vinylpyridine copolymer (pNIPVP) hydrogel spheres. Due to the presence of poly(4-vinylpyridine) moieties, the pore size of the gel network can be manipulated by varying the pH of the system, which was used to uptake and then fix the CdTe nanocrystals within the polymer matrix. Furthermore, multicolor-coded microspheres can be realized by simultaneously incorporating two different CdTe nanocrystals into the spheres.[94]

By utilizing the inherent temperature-dependent volume phase transition of the pNIPAM hydrogel, we were also successful in preparing fluorescent polymer spheres incorporated with CdTe nanocyrstals co-stabilized by TGOL and TGA.[95] As a result of hydrogen bonding established between the hydroxyl group of TGOL on the surface of the nanocrystals and the amide groups from the pNIPAM gel networks, the CdTe nanocrystals are effectively trapped within the pNIPAM spheres, resulting in highly fluorescent microspheres as shown in Fig. 6. It was further demonstrated that the temperature-dependent volume phase transition still persists in the final composite spheres even though it is greatly weakened, which however allows further decreasing the distance between differently sized CdTe nanocrystals by increasing the temperature. In this way, an average distance required for Förster energy transfer was estimated. Simultaneously loading different phosphors within single beads has been demonstrated to be an effective approach for readily creating fluorescent beads with pre-designed colors simply by varying the ratio of different phosphors.[95] Nevertheless, it is most important prerequisite to effectively avoid the energy transfer process, as it will introduce optical impurities to the resultant beads.

The above-mentioned pNIPAM systems offer excellent opportunities for proof-of-concept studies in achieving fluorescent polymer beads by loading them with pre-formed CdTe nanocrystals. However, the use of porous beads as matrices may also enhance the nonspecific adsorption of analytes. Most importantly, the diffusion of oxygen and water from the surrounding media into the composite beads will accelerate the photodegradation of the CdTe nanocrystals. Therefore, hydrophobic matrices possessing a compact structure are more suitable for achieving robust fluorescent microbeads. An easy way to achieve this goal is to directly polymerize hydrophobic radical monomer droplets containing organic soluble semiconductor nanocrystals.[96,97] However, two bottlenecks need to be overcome in this route, namely, the aggregations of inorganic nanoparticles caused by mutual incompatibility between the organic polymer and inorganic nanoparticles,[96–102] and the effective encapsulation of the inorganic nanoparticles within the polymeric beads.[96,97,103] In addition, to preserve the fluorescence of the original semiconductor nanocrystals incorporated is also challenging since some radicals can heavily quench the fluorescence of the semiconductor nanocrystals.[96,97]

We have previously demonstrated that the use of polymerizable surfactant to transfer the aqueous CdTe nanocrystals to the styrene phase is an effective solution for overcoming the aggregation of CdTe nanocrystals caused by mutual incompatibility between the resultant polystyrene (PS) and the incorporated inorganic nanocrystals.[104] Following on from these early investigations, we have been successful in preparing multiplexed optical encoding polystyrene beads incorporated with MPA-capped CdTe nanocrystals *via* a modified miniemulsion polymerization method.[96,97] Apart from didecyl-*p*-vinylbenzylmethylammonium chloride (DVMAC) which was used as phase transferring agent, octadecyl-*p*-vinylbenzyldimethylammonium chloride (OVDAC) was also designed and used as emulsifier in combination with Triton X-100. In comparison with the convention surfactants, the polymerizable feature of OVDAC enabled an effective encapsulation of the CdTe nanocrystals in the final composite spheres, as shown in Fig. 7.[96] Further investigations demonstrated that the hydrophobic nature and compact structure of

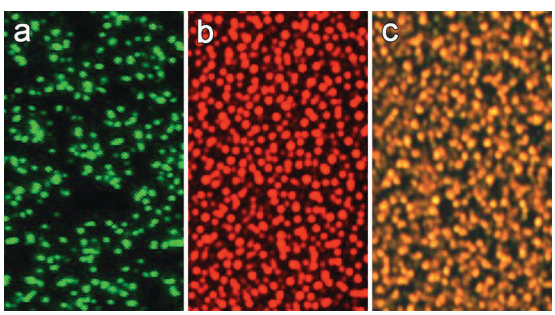

Fig. 6 Fluorescence images of pNIPAM microspheres loaded with 2.5 nm CdTe nanocrystals (a), 3.5 nm CdTe nanocrystals (b), and the mixture of these two nanocrystals with a molar ratio of 5 : 1 (2.5 nm CdTe to 3.5 nm CdTe) (c). These microspheres were prepared by incubating the nanocrystals and gel spheres at 45 °C. The fluorescence images were captured at room temperature (reprinted from ref. 95).

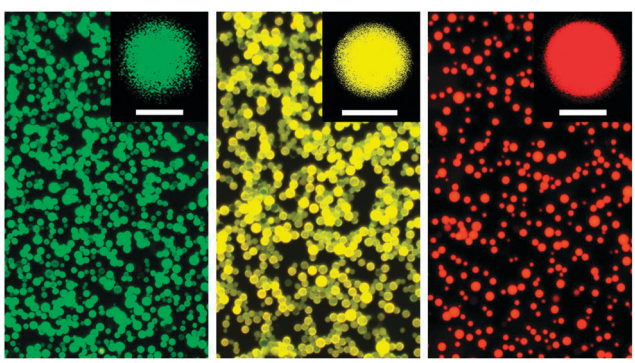

Fig. 7 Fluorescence images of polystyrene beads loaded with green (left), yellow (middle), and red fluorescence CdTe nanocrystals (right). The insets are the corresponding confocal fluorescence images. The scale bars correspond to 2 μm (reprinted from ref. 96).

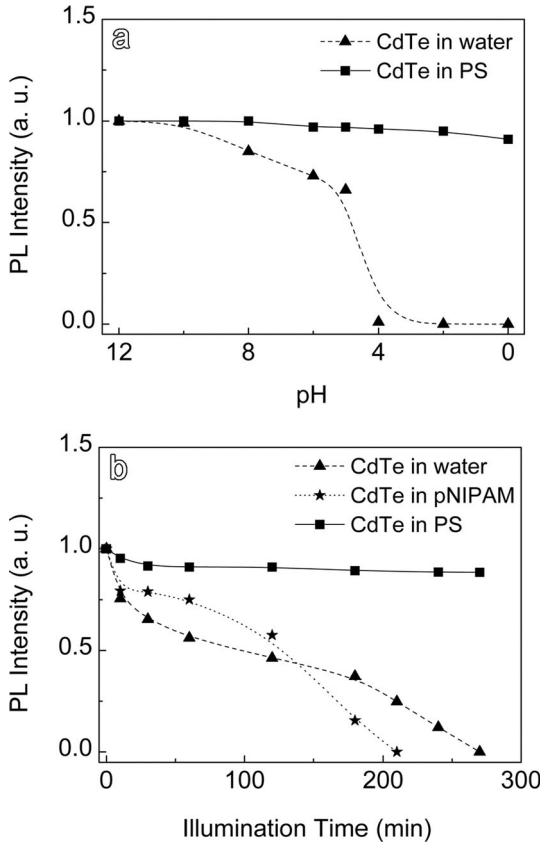

Fig. 8 (a) pH dependency of the fluorescence of CdTe nanocrystals in water or incorporated PS beads suspended in water; (b) The photostability of red fluorescence CdTe nanocrystals in water, in pNIPAM microspheres, and in PS beads suspended in O_2-aerated water (reprinted from ref. 96).

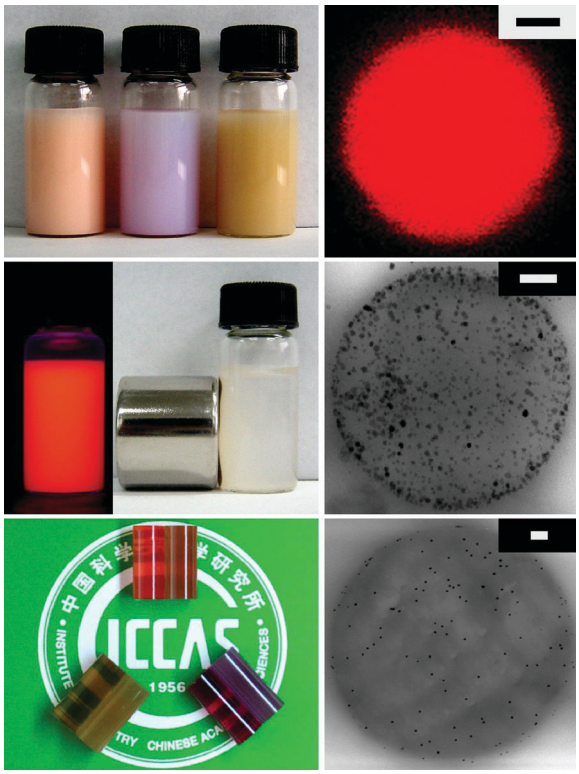

Fig. 9 The top left image was taken from aqueous dispersions of CdTe@PS (left), Au@PS (middle), Fe_3O_4@PS (right) beads. The middle left images were taken from the CdTe@PS bead solution under UV light (left) as well as the Fe_3O_4@PS bead suspension after it was put near to a permanent magnet for minutes (right). The bottom left image presents three pairs of NPs/PS composite monoliths prepared using DVMAC (left) and DEMAC (didecyl-*p*-ethylbenzylmethylammonium chloride) (right) as phase transfer agents, respectively. The monoliths shown clockwise are CdTe/PS (top), Au/PS and Fe_3O_4/PS. The top right image was taken from a single CdTe@PS bead by confocal fluorescence microscopy. The fluorescence efficiency of the CdTe@PS bead was estimated to be 17%. The middle right and bottom right photographs are cross-sectional TEM images taken from thin slices of Fe_3O_4@PS and Au@PS beads, respectively. The scale bar in the right-hand images corresponds to 100 nm. The initial concentrations of CdTe, Fe_3O_4 and Au particles in the styrene solutions were 6.4×10^{-5}, $1.1 \times 10^{-6}$and 1.8×10^{-7} M, respectively (reprinted from ref. 97).

the PS matrix allows robust fluorescent beads whose fluorescence efficiency is nearly pH-independent, as shown in Fig. 8a.[96] Additionally, the polymerizable emulsifier DVMAC help to firmly hold the CdTe nanocrystals against the good solvent styrene. Though the fluorescence efficiency of resultant CdTe-PS microspheres is around 8–17% which was decreased by a factor of 1.7–2.0 in comparison with that of the original CdTe nanocrystals, under continuous UV irradiation, the encapsulated CdTe nanocrystals are much more stable than the original nanocrystals in neutral water and those incorporated in pNIPAM spheres, as shown in Fig. 8b, which further verify the idea of encapsulating fluorescent nanocrystals in hydrophobic polymers for achieving robust fluorescent beads.[96]

The novelty of using polymerizable surfactants as both emulsifier and phase-transfer agent was further manifested by investigations on encapsulating different types of aqueous nanocrystals, such as Fe_3O_4 nanocrystals as a representative of metal oxide nanoparticles, and Au nanocrystals as a representative of noble metal particles, in PS beads prepared by the modified miniemulsion polymerization method developed by Gao's group (Fig. 9).[97] Following these investigations, Wu and co-workers also succeeded in preparing fluorescent beads incorporated with polyoxometalates.[105]

4. Preparation of low-dimensional CdTe nanostructures

In addition to the zero-dimensional CdTe dots, one-dimensional CdTe nanorods and nanotubes can also be synthesized through the aqueous synthetic routes. Moreover, CdTe nanowires,[49] twisted ribbons,[50] two-dimensional CdTe nanosheets[106] and even three-dimensional CdTe aerosol[107] are also obtained based on the thiol-capped CdTe nanocrystals.

4.1 Preparation of one-dimensional CdTe nanostructures

Preparation of low-dimensional CdTe nanostructures with different morphologies in liquid phase is recently receiving increasing attention.[39,48–50,108,109] So far, CdTe nanorods or tetrapods achieved *via* the pyrolysis of organometallic

precursors in organic solvents have been reported by properly controlling the growth kinetics of CdTe.[110,111] Nevertheless, the progress on the morphological control over II–VI nanocrystals synthesized in aqueous solutions is less developed, due to the interference of water which inevitably acts as a coordinating solvent in the aqueous synthetic route. Li *et al.* first observed CdTe nanorods formed in aqueous solution by using mixed ligands cysteine and TGA.[109] Latterly, Zhang *et al.* performed systematic investigations on CdTe nanorods prepared *via* the aqueous synthetic route.[48,112] They demonstrated that an appropriate aging process at a temperature lower than 80 °C is necessary for converting the thiol-capped CdTe clusters to one-dimensional CdTe nanorods. Moreover, a suitable structure of the surface-capping thiol molecules is essentially required. Only TGA and its derivatives can lead to CdTe nanorods. The authors attributed the anisotropic growth of CdTe to the secondary coordination between the carboxyl group of TGA or its derivatives and the primary thiol-coordinating cadmium.[48]

As a matter of fact, the secondary coordination between TGA and cadmium ion can lead to rather complicated stoichiometric complexes.[31,39] For example, by refluxing the typical precursor solution containing $Cd(ClO_4)_2$ and TGA with a feeding molar ratio of 1 : 1, we for the first time observed super-long nanowires with a helical belt structure as shown in Fig. 10.[39] As a matter of fact, cadmium thiolates have been intensively investigated. One-dimensional complex structures formed by cadmium ions and various types of thiol ligands have been found in the macrocrystals of cadmium coordination polymers.[38,113,114] Typically, the molar ratio of cadmium to thiol ligand in such linear coordination polymers is universally 1 : 2; that is, cadmium atoms are linked by pairs of doubly bridging thiolate ligands. However, additional coordination may also exist depending on the structure of the thiol molecules. For example, Dance *et al.* demonstrated that in the linear chain structures formed by $[Cd^{II}(\mu\text{-}SCH_2COOCH_2CH_3)_2]$, the primary coordination of each cadmium atom is $Cd(\mu\text{-}SR)_4$. In addition, four carboxylic oxygen atoms coordinate with cadmium forming dodecahedrons alternated by tetrahedrons of $Cd(\mu\text{-}SR)_4$.[38] According to their calculations, the two CdS_2 primary coordination planes in the dodecahedron are almost orthogonal (87.1°). As TGA is structurally very similar to $HSCH_2COOCH_2CH_3$, it is reasonable to believe that Cd-TGA complexes also possess similar coordination structures in which the non-perpendicular intersection between the two adjacent CdS_2 primary coordination planes along each single Cd-TGA polymer chain introduces the helical belt structure to the one-dimensional aggregates formed by Cd-TGA polymers. Following this structural analysis, poly(acrylic acid) was successfully used to tune the diameter of the one-dimensional nanostructure formed by the CdTe-TGA complex upon weak intermolecular interactions. Further experiments demonstrated that the one-dimensional nanostructures can be used as precursors, independent of their diameter, for producing superlong CdTe nanotubes (Fig. 11) upon further reactions with NaHTe, suggesting that the formation of CdTe nanotubes generally follows the mechanism for the sacrificial template approach, as the Cd-TGA complex is a common precursor for CdTe nanocrystals. It is also demonstrated that upon reaction with Na_2S, the Cd-TGA nanowires can be converted into CdS nanotubes. Thereupon, *via* cation exchange reaction by using the CdS nanotubes as template, HgS nanotubes can also obtained.[39] Following these results, Murase and co-workers recently reported fluorescent CdTe fibers prepared by the conventional aqueous synthetic route for TGA-capped CdTe nanocrystals, except that TEOS was introduced in the reaction system, so as to achieve $CdTe@SiO_2$ hybrid materials.[115]

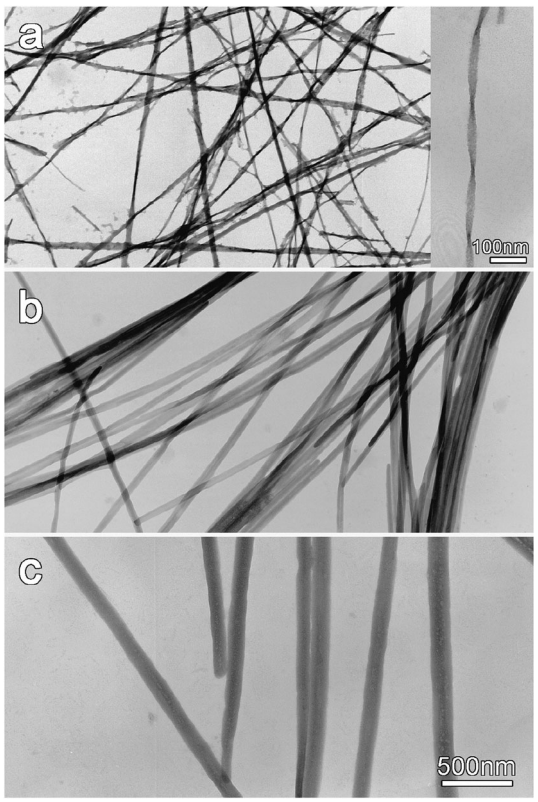

Fig. 10 TEM images of one-dimensional Cd-TGA nanowires prepared in the absence of polyacrylic acid (PAA) (a), and in the presence of PAA at Cd : TGA : AA (acrylic acid unit) molar ratios of 1 : 1 : 0.1 (b), and 1 : 1 : 0.3 (c). The inset in panel (a) shows the helical belt structure in the nanowires formed in the absence of PAA (reprinted from ref. 39).

In addition to the direct synthesis of one-dimensional CdTe nanorods and nanotubes, Tang and Kotov have demonstrated that CdTe crystalline nanowires can also be obtained through the spontaneous reorganization of TGA-capped CdTe nanocrystals after controlled removal of the surface-capping thiols. Since the diameter of the resultant CdTe nanowires is virtually identical to the diameter of the original nanocrystals, it can be controlled by using CdTe nanocrystals of difference sizes.[49]

More recently, this group further reported twisted ribbons formed upon the self-assembly of TGA-capped CdTe nanocrystals under controlled illumination.[50] Different from the former reports, in this study, the CdTe nanocrystals were prepared with the TGA to Cd^{2+} ratio close to 1.0, rather than the commonly used ratio of 2.4 : 1. The authors claimed that tellurium ions in CdTe nanocrystals can be slowly oxidized under this condition. Consequently CdTe nanocrystals are

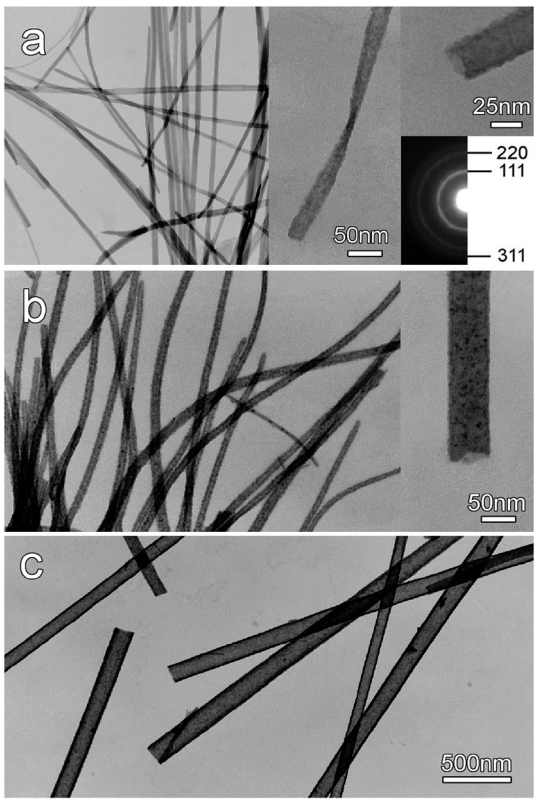

Fig. 11 TEM images of CdTe nanotubes obtained by introducing NaHTe into aqueous dispersions of the nanowires shown in Fig. 10. The insets show TEM images taken under higher magnifications as well as an electron diffraction pattern of the nanotubes presented in (a) (reprinted from ref. 39).

converted to CdS-dominant nanocrystals, which prevents the CdTe nanocrystals from recrystallizing into thin, cylindrical nanowires as they reported before, because CdS has a greater activation barrier of recrystallization. Moreover, the authors found that the twisted ribbons can only be induced by illumination with visible light, and can be controlled by both intensity and the time of light exposure. They claimed that the twisting structure is produced as a result of internal shear strain introduced by the photocorrosion of the individual nanoparticle units.[50]

4.2 Preparation of two- and three-dimensional structures based on CdTe nanocrystals

Following from one-dimensional CdTe nanowires, Tang and Kotov latterly reported two-dimensional free-floating CdTe sheets formed by the self-assembly of 2-(dimethylamino)-ethanethiol-capped CdTe nanocrystals.[106] Since DMAET (2-(dimethylamino)ethanethiol) possesses two hydrophobic methyl groups and can also be positively charged *via* the protonation of the dimethylamino group, it is believed that anisotropic electrostatic interactions arising from both a dipole moment and a small positive charge, combined with directional hydrophobic attraction, are responsible for the formation of the two-dimensional free-floating nanosheets.[106]

Different from the self-assembled one-dimensional CdTe nanowires and two-dimensional CdTe nanosheets, Gaponik and co-workers found that TGA-capped CdTe nanocrystals can also form gel-like precipitates from aqueous colloidal solutions upon storage of 1–2 years in the dark. The author attributed this spontaneous gelation to a slow stabilizer oxidation by oxygen present in the colloidal solution or hydrolysis of the thiol stabilizers at high pH values.[107] Following this finding, the authors further developed a reproducible and controllable method to assemble the TGA-capped CdTe nanocrystals into a three-dimensional hydrogel based on chemical destabilization and photochemical treatment of the TGA-capped CdTe nanocrystals. Thereupon, the three-dimensional fluorescent CdTe aerogel was prepared by exchanging the interstitial solvents with acetone as a transition fluid.[107]

Very recently, this group further demonstrated that the TGA-capped CdTe nanocrystals can self-assemble into three-dimensional hybrid nanostructures upon a heating treatment of an aqueous solution containing CdTe nanocrystals, ethanol and sodium acetate.[116] Different from the former CdTe gel, three-dimensional nanostructures are formed by entangled nanowires consisting of both CdTe nanocrystals and Cd-TGA complexes. The formation of Cd-TGA nanowires can be understood by the fact that the TGA molecules partly depleted from the surface of CdTe nanocyrstals by ethanol will react with the extra Cd^{2+} in the mother-solution to form Cd-TGA nanowires, as reported by Gao and co-workers. Since residual TGA molecules on the surface of the CdTe nanocrystals also have a chance to coordinate with Cd^{2+} in the Cd-TGA complexes, three-dimensional structures of entangled Cd-TGA nanowires incorporated with CdTe nanocrystals are formed.[116]

5. Applications of CdTe nanocrystals

The unique optical properties make the CdTe nanocrystals potentially useful in electroluminescence devices, metal ion sensing, immunoassays, cell labeling and *in vivo* imaging for tumor detection. As the applications of CdTe nanocrystals in metal ion sensing and immunoassays have recently been reviewed,[28,117] it will not be included herein.

5.1 Electroluminescence of CdTe nanocrystals

II–VI semiconductor nanocrystals are of great technological interest as emitting materials for thin film electroluminescence (EL) devices.[27] In general, the semiconductor nanocrystals exhibit many unique properties which are promising for the improvement of EL devices. (1) The color of emission can easily be tuned by varying the size of the nanocrystals, while their chemical properties remain nearly the same. Therefore, one device fabricating procedure can be adopted for different size nanocrystals so as to produce different color EL emissions.[118–120] (2) The high fluorescence efficiency achieved by careful surface modification should be greatly in favor of the device efficiency.[23,121–124] (3) The thermal stability of inorganic nanocrystals is expected to be higher than that of organic materials. (4) The recombination of charge carriers in semiconductor nanocrystals is not restricted by the spin statistics. The energy of the lowest exciton state of the particles is split by only a few meV into different levels for different mutual spin orientations of the electron or hole states.[125] Therefore, even if charge carriers form a forbidden spin

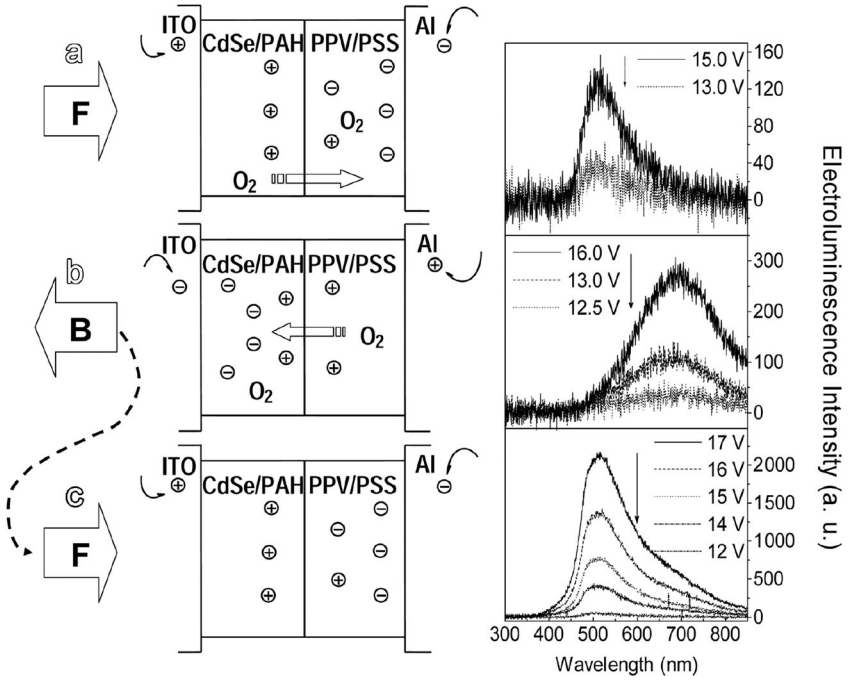

Fig. 12 Schematic drawings of the structure of an ITO||PEI(CdSe/PAH)*10*|(PSS/PPV)*10*||Al two-layer composite film EL device (left). EL spectra of the composite film devices recorded at room temperature in air (right). The EL spectra recorded from a fresh sample under forward bias are presented in the top frame. The EL spectra recorded from a fresh sample under backward bias are presented in the middle frame, and the EL spectra recorded under forward bias after the device was first operated under backward bias are shown in the bottom frame (reprinted from ref. 138).

combination, it can easily be brought back to a radiative state by thermal activation.[126]

Different from organic soluble nanocrystals which can be blended with conducting polymers *via* solution processes performed in organic solvents,[120] the aqueous nanocrystals however can be assembled into solid-state films by ionic layer-by-layer (LbL) self-assembly processes taking place in aqueous media, which is obviously more environment-friendly.[127] The ionic LbL self-assembly technique has been demonstrated to be a very simple approach for combining semiconductor nanocrystals with various organic materials in forming homogenous ultrathin films, which has been summarized in a large number of review articles, especially in recent ones by Gaponik,[128] Eychmüller,[129] and Kotov.[130] Moreover, the ionic LbL self-assembly technique allows the buildup of multilayer structures in which different types of materials are precisely layered along the film normal direction, which is especially advantageous for the construction of electro-optical devices.[27]

The ionic LbL self-assembly technique paved by Decher and Möhwald has been proven to be a facile approach for producing high quality ultrathin films.[127,131] Utilizing alternate adsorptions of negatively charged inorganic nanoparticles and positively charged rigid bipolar amphiphiles or positively charged polyelectrolytes, the LbL self-assembly technique has been demonstrated to be feasible for embedding aqueous nanoparticles in organic matrices by Gao[37,100,132,133] and Kotov[134–136] in early reports. Following on the early works, Gao *et al*. did systematic investigations on EL of LbL self-assembled films containing CdSe and CdTe nanocrystals synthesized *via* the aqueous synthetic route.[137–142]

Different from CdTe nanocrystals, CdSe nanocrystals stabilized by thiolactic acid (TLA) present surface-trap-dominant fluorescence which is characterized by a very broad whitish photo-emission.[138,143] By assembling TLA-capped CdSe nanocrystals and a positively charged precursor of poly-(*p*-phenylene-vinylene) (pre-PPV) *via* the LbL self-assembly technique, EL devices with a device structure of ITO||-PEI(CdSe/PPV)*20*||Al (PEI = poly(ethyleneimine)) were constructed after converting pre-PPV to PPV which is a well-known conducting polymer. EL was successfully observed from such 20 bilayer CdSe/PPV ultrathin film devices although the external quantum efficiency remained low.[143]

Taking advantage of the ionic LbL self-assembly technique in fabricating complex structures by placing different materials at various film normal positions, Gao *et al*. further investigated EL of two-layer devices constructed by stacking 10-bilayer PSS/PPV (PSS = poly(styrenesulfonic acid) self-assembled film on the top of 10-bilayer CdSe/PAH (PAH = poly(allyl-amine) hydrochloride) self-assembled film pre-deposited on ITO.[138] Herein, each layer with respect to the structure of an EL device consists of *n* bilayer LbL self-assembled films of different materials denoted as (N/P)*n*. After depositing an aluminum electrode on the ultrathin composite film, the final two-layer devices were obtained and denoted as ITO||PEI(CdSe/PAH)*10*|(PSS/PPV)*10*||Al. The EL behaviors of such two-layer devices were carefully investigated by comparing with single-layer devices consisting of 20-bilayer CdSe/PAH or 20-bilayer PSS/PPV. The following extraordinary behaviors were observed. (1) The radiative recombination zone of electrically injected charge carriers can be controlled

by the direction of external bias, *i.e.*, a forward bias leads to EL of PPV while a backward bias gives rise to EL of CdSe nanocrystals, as shown in Fig. 12. In other words, the same device can generate EL of two different colors dependent on the bias direction. (2) The bias direction applied on a device freshly prepared under ambient conditions has strong impact on the lifetime of PPV EL. This is because trace oxygen enclosed in the device can be scavenged by CdSe nanoparticles when the recombination zone of charge carriers is firstly located in the CdSe/PAH layer driven under backward bias. In this way, the EL of PPV achieved subsequently by forward bias can greatly be enhanced by at least one order of magnitude.[138]

In spite of the extraordinary effects of CdSe nanocrystals acting as oxygen scavenger in the two-layer EL device, further applications of CdSe nanocrystals in EL devices is limited by the broad optical emission of the thiol-capped CdSe nanocrystals synthesized through the aqueous synthetic route.[19,138] Therefore, in subsequent investigations, Gao *et al.* adopted TGA-capped CdTe nanocrystals to replace CdSe nanocrystals in fabricating similarly structured LbL self-assembled films[144] and EL devices.[139,141] Several commonly used positively charged polyelectrolytes such as PEI, PAH and PDDA (poly(diallyldimethylammonium chloride)) were used to optimize the fluorescence of the resultant films.[144] On the basis of these investigations, PDDA was chosen to fabricate CdTe/PDDA films and EL devices.[139,141] Owing to the strong size-dependent fluorescence, EL of different colors well correlating to the fluorescence of CdTe nanocrystals was achieved with room-light visible light output, as shown in Fig. 13. The external quantum efficiency of the EL device was estimated to be around 0.1%. The EL devices were characterized by a very low onset voltage of 2.5–3.5 V, much lower than similarly structured (CdSe/PAH)**n* devices,[141] which suggests that the energetic levels of CdTe nanocrystals match the work functions of ITO and aluminum electrodes better than CdSe nanocrystals, leading to lower energy barriers for charge carrier injections. In addition, particle size dependence of EL efficiency was also observed and explained by the size-dependent shifts of the CdTe energetic levels with respect to the work functions of the electrodes.[141]

Recently, Eychmüller and co-workers reported quite similar results on EL of (CdTe/PDDA)**n* LbL self-assembled films but with an improved external quantum efficiency of around 0.5%.[145] Nevertheless, there is no reason to take this efficiency as the upper limit of the CdTe nanocrystal-based EL devices. By use of the ionic LbL technique, Marchese and co-workers developed a novel all-inorganic EL device consisting CdTe nanocrystals. The films were prepared by alternate depositions of CdTe nanocrystals and a layered double hydroxide (LDH) hydrotalcite-like material. 20-bilayer CdTe/LDH self-assembled films were prepared and used for constructing an EL device of ITO||(CdTe/LDH)**20*||Al. Apart from low turn-on voltage of 3–4 V, this new type of EL device is characterized by excellent thermal stability, benefiting from the full inorganic components.[146]

As aforementioned, the ionic LbL self-assembly technique is a low cost and green approach for fabricating EL devices of different CdTe nanocrystals. In addition, it offers a high degree of control over different types of materials along the film normal direction. However, to achieve multicolor displays based on the self-assembled films of CdTe nanocrystals, lateral patterning of multiple CdTe nanocrystal films is an important prerequisite. Towards this goal, Gao and Feldmann developed an electric field directed layer-by-layer assembly (EFDLA) method by which the LbL self-assembled films consisting of different types of functional materials can be deposited on different locations of a conducting substrate.[142,147–149] The basic idea is to use an electric field to direct a location-selective deposition of the LbL self-assembled films. By this EFDLA method, binary patterned arrays of self-assembled films consisting of two differently sized CdTe nanocrystals were fabricated by a two-step deposition to demonstrate the feasibility of this novel method. The resultant 2 mm wide binary patterned arrays shown in Fig. 14 present a huge fluorescence contrast. By evaporating aluminum through a mask with 2 mm wide gaps perpendicularly aligned to the film stripes, the PDDA/CdTe films were sandwiched in between, forming two 2 × 2 mm electroluminescence pixels which were demonstrated to emit light of different colors under a forward bias of 5 V. These results suggest that the EFDLA method may open up an elegant way toward nanocrystal multicolor displays[147] or multi-analyte sensing.[148]

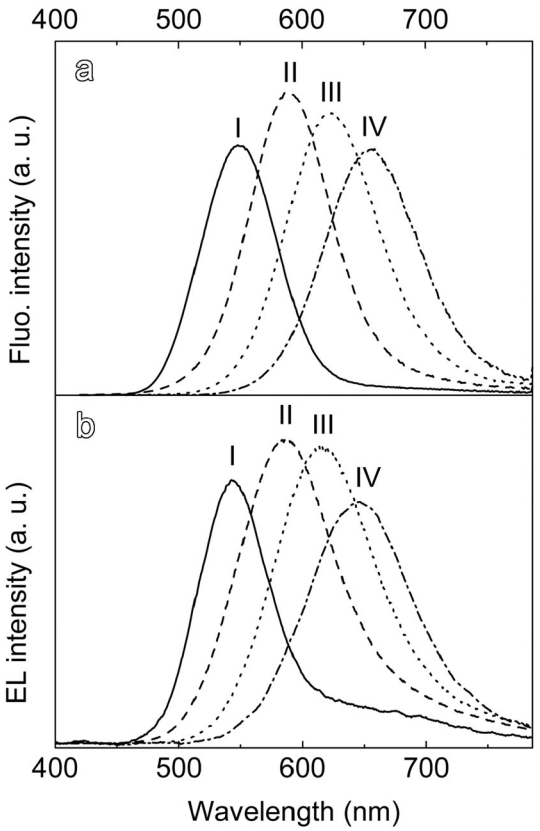

Fig. 13 Frame a shows fluorescence spectra of aqueous solutions of four different CdTe nanocrystals (I, II, III, IV) recorded by excitation at 400 nm. Frame b presents electroluminescence spectra of 30 bilayer CdTe/PDDA film devices of these four nanocrystals (reprinted from ref. 141).

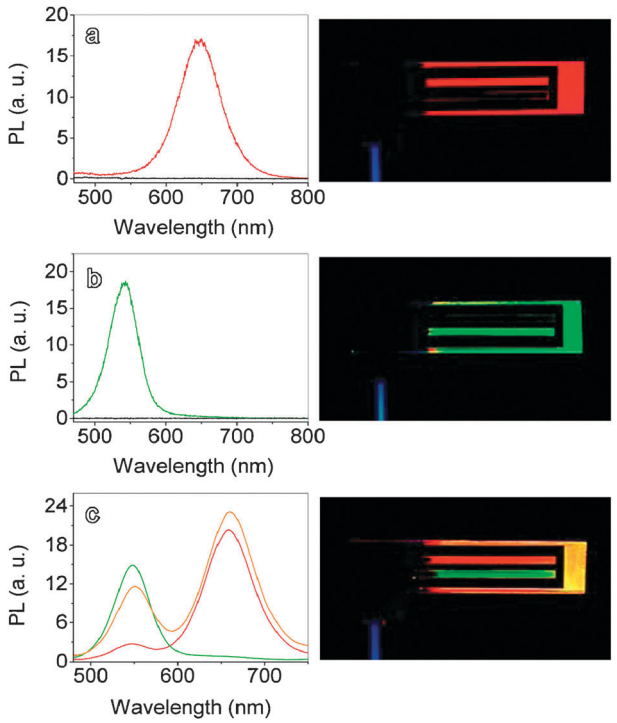

Fig. 14 Photographs of the lateral structures of EFDLA films of CdTe nanocrystals with green emission (CdTe_green) and red emission (CdTe_red): (a) (PDDA/CdTe_red)*40*, (b) (PDDA/CdTe_green)*40*, and (c) (PDDA/CdTe_red)*40*||(PDDA/CdTe_green)*60*. The fluorescence spectra recorded from the electrodes as well as the marginal area for the sample on the bottom are shown in the left-hand frames (reprinted from ref. 147).

5.2 Bioapplications of CdTe nanocrystals

Apart from being useful in optoelectronic devices, II–VI semiconductor nanocrystals are also considered to be a new class of materials for various bioapplications owing to their unique optical properties. Since Alivisatos and Nie independently reported their investigations on CdSe nanocrystal-based bioprobes,[6,7] the applications of fluorescent nanocrystals in different biological and biomedical fields have received increasing attentions over the past decade.

In comparison with the highly fluorescent CdSe nanocrystals produced in the organic phase *via* the TOP-TOPO method, the mercapto acid-stabilized CdTe nanocrystals synthesized through the aqueous synthetic route can more facilely be used for binding with biomolecules. In 2002, Kotov and co-workers reported CdTe-protein probes prepared by covalently conjugating two different CdTe nanocrystals to bovine serum albumin (BSA) and anti-BSA antibody (IgG), respectively. Upon the antigen–antibody recognition, BSA-IgG immunocomplexes were formed and Förster resonance energy transfer (FRET) between two different CdTe nanocrystals was observed.[150] Since then, CdTe nanocrystals have been used to couple with antibodies, DNA, peptides or other types of bioligands in fabricating versatile bio-probes useful for immunoassays, cell labeling and *in vivo* imaging.[28–30,117,151–153]

However, no matter what types of bioligands are conjugated to the fluorescent nanocrystals, the binding specificity of the resultant probes is often interfered with the non-specific interactions between the particles and the receptors.[152] With respect to cell labeling applications, the interactions of nanoparticles with both cell membrane and membrane proteins are mainly responsible for the non-specific binding of the nanoprobes. Poly(ethylene glycol) (PEG) is a widely used biocompatible polymer known to have good resistance to the nonspecific bindings with biotargets.[154–160] Gao and co-workers have demonstrated that appropriate PEG modification on CdTe nanocrystals can greatly suppress the non-specific interactions between CdTe nanocrystals and cancer cells.[152] The PEG coating was achieved *via* a ligand exchange process by mixing MPA-capped CdTe nanocrystals in PBS buffer with a thiolated PEG (M_n = 750) prepared through a reaction between NH_2-PEG and 2-iminothiolane hydrochloride. In the following experiments, they observed that the anti-carcinoembryonic antigen monoclonal antibody rch 24 (rch 24 mAb) presented very strong affinity to the PEG-modified CdTe nanocrystals, which is quite probably caused by the imine and secondary amine residues in the thiolated PEG. The resultant fluorescent CdTe-(rch 24 mAb) conjugates presented a satisfactory binding specificity to CEA-positive carcinoma cells in contrast to CEA-negative cells. In comparison to the widely used FITC, the CdTe nanocrystal-based fluorescence probes exhibited much better stability under illumination in addition to brighter fluorescence.[152]

Apart from the applications in specific cell membrane protein labeling, CdTe nanocrystals are also potentially useful for visually tracking the intracellular biological processes due to their excellent stability against photo-bleaching. In fact, fluorescent II–VI semiconductor nanocrystals have been used in recent gene studies.[161–171] For example, in one of the earlier investigations, CdSe@ZnS core/shell nanocrystals were used to detect a gene silencing effect after being co-transfected with small interfering RNA (siRNA) using cationic liposomes, upon an assumption that the fluorescence intensity of the nanocrystals loaded by cells is directly correlated with the biological effects of siRNA.[161] By attaching plasmid DNA on CdSe@ZnS core/shell nanocrystals *via* a specific interaction between PNA (peptide nucleic acids) on the nanocrystals and plasmid DNA, Burgess and co-workers developed a fluorescent probe for intracellular tracking of the plasmid DNA after the probe was delivered using cationic liposomes.[162] Jia *et al.* adopted TGA-capped CdTe nanocrystals to covalently label an antisense oligodeoxynucleotide (ASON) and further developed a gene delivery system by using multiwall carbon nanotube as carriers. The intracellular transport of ASON was optically visualized by the fluorescence of CdTe nanocrystals.[172]

The effective delivery of genes into cells is undoubtedly one of the most important steps towards gene transfection. However, the following endosomal escape, cytoplasmic mobility, and nuclear entry of foreign genes are also very important for *in vitro* gene transfection with respect to non-viral gene transfection systems.[173] Therefore, to visually track and identify the intracellular localization of a foreign gene would be greatly helpful for revealing the intracellular target sites of the transfected genes for elucidating the biological actions and processes exerted or caused by the transfected genes, and thereby probing the mechanisms of the transfected

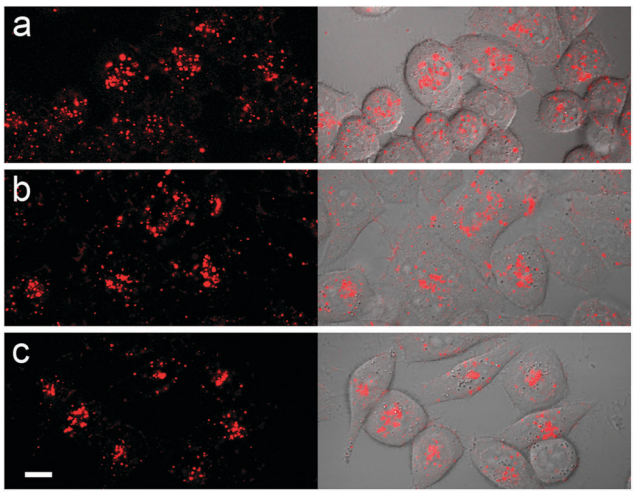

Fig. 15 Dark and merged field images of HeLa cells obtained after incubation for 60 min with CdTe-A5 (a), CdTe-A29 (b), and CdTe-A40 (c), respectively (A5: 5′-NH_2-AAA AA; A29: 5′-NH_2-AAA AAA AAA AAA AAA AAA AAA AAA AAA AA; A40: 5′-NH_2-AAA AAA AAA AAA AAA AAA AAA AAA AAA AAA AAA AAA A). The scale bar in the micrograph corresponds to 10 μm (reprinted from ref. 153).

genes at the cellular level. Very recently, Gao and co-workers successfully developed a fluorescent system by covalently conjugating anti-survivin ASON to TGA-capped CdTe nanocrystals for gene transfection and intracellular visualization of transfected genes.[153] It was found that the oligonucleotides, independent of their base sequence and length, can promote effective cellular uptake of the resultant CdTe-oligonucleotide conjugates, as shown in Fig. 15. Systematic investigations revealed that the cellular uptake of the negatively charged CdTe-oligonucleotide conjugates is through the macropinocytosis pathway. Most importantly, the ASON covalently attached to the surface of CdTe nanocrystals can still exert its biological functions after cellular uptake, *i.e.* it can specifically down-regulate the survivin mRNA and ultimately induce the apoptosis of the HeLa cells. As expected, the intracellular localization of the CdTe-ASON probes can visually be tracked. In contrast to the control probe composed of the suvivin sense oligonucleotides (SON) and CdTe nanocrystals, the CdTe-ASON probes mainly localize in the cytoplasm but showing a tendency of being accumulated around the nucleus, as shown in Fig. 16, while most of CdTe-SON conjugates accumulate in the nucleolus with the remainder being arbitrarily distributed within the cells. This is the first time observation on the specific intracellular localization of antisense oligonucleotides, and these results imply that the perinuclear region might be the location where the antisense regulation process occurs. Because the down-regulation of survivin mRNA induced by ASON ultimately leads to the apoptosis of HeLa cells, the accumulation of the CdTe-ASON probes in the perinuclear region—visualized through fluorescence—may specifically indicate the early stages of apoptosis induced by survivin deficiency.

Very recently, TGA-capped CdTe nanocrystals were also used in investigations of the biological barrier in human skin.[174] By monitoring the fluorescence of CdTe nanocrystals in different depth of skin, it was concluded that the stratum corneum is the main barrier for CdTe nanocrystals penetrating through human skin, and only when the stratum corneum is partly damaged, the CdTe nanocrystals can penetrate into deeper layers of human skin.[174]

Apart from *in vitro* applications, CdTe nanocrystals are also useful as fluorescence probes for *in vivo* imaging.[29,30] For example, a novel nanocarrier of drugs was developed upon spontaneous self-organization of positively charged PEI (or pegylated PEI) and negatively charged MPA-capped CdTe nanocrystals together with the negatively charged model drug plasmid DNA. Benefiting from the fluorescence of the CdTe nanocrystals, the biodistribution of the plasmid DNA was successfully tracked and the fluorescent signal remained detectable for at least a week.[30] For *in vivo* tumor detection, pegylated phospholipid micelle was used to encapsulate CdTe@ZnSe core/shell nanocrystals synthesized upon the aqueous synthetic route. Then peptide cRGD (cycl (Arg-Gly-Asp-D-Phe-Cys)) as tumor-specific ligand was covalently conjugated to the fluorescent micelle. The resultant nanoprobes exhibited certain binding specificity in imaging integrin $\alpha_v\beta_3$ overexpressed on the tumor vasculature.[29]

Cytotoxicity is however an important issue that cannot simply be parried away with respect to the bioapplications of cadmium chalcogenide nanocrystals. The cytotoxicity of CdTe nanocrystals is believed to arise from the released Cd^{2+}.[175,176] Moreover, it was found out that the electron–hole pairs formed upon excitation of semiconductor nanocrystals could undergo electron transfer to oxygen leading to the formation of reactive-oxygen species, which may also be involved in the cytotoxicity of CdTe nanocrystals.[176] Until now the cytotoxicity of CdTe nanocrystals remains far from being completely understood due to the complexity of the related mechanisms. Nevertheless, development of suitable coating techniques, should be the only measure required for solving the toxicity problem.

6. Remarks and perspectives

Owing to a suitable bandgap, CdTe offers another platform for achieving highly fluorescent nanomaterials comparable to CdSe nanocrystals synthesized in organic phase based on the TOP-TOPO method. After 20 years effort, the aqueous synthesis of highly fluorescent zero-dimensional CdTe nanocrystals has become increasingly mature, even though water as a strong polar coordinating solvent introduces unavoidable and complicated chemistry into the aqueous synthesis. Along with the development of the aqueous synthetic route for CdTe nanocrystals, the use of water-soluble thiol ligands, especially mercapto acids, has been demonstrated to be one of the most important steps towards highly fluorescent CdTe nanocrystals with well-defined optical properties. Moreover, the special coordination between TGA and Cd^{2+} leads to many unexpected CdTe nanostructures such as zero-dimensional CdTe@Cd-TGA core/shell particles, one-dimensional CdTe nanowires and nanotubes, and three-dimensional self-assembled structures comprised of entangled CdTe@Cd-TGA hybrid nanowires. In addition, by properly detaching the surface binding thiols

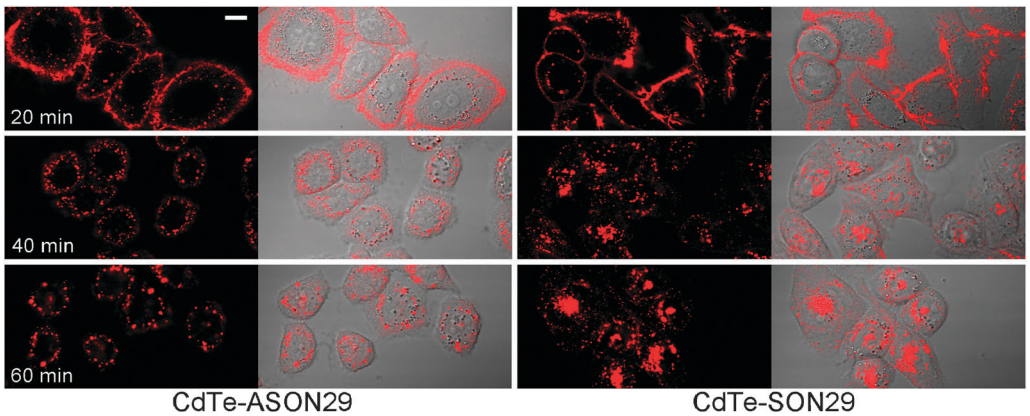

Fig. 16 Dark and merged field images of HeLa cells incubated with CdTe-ASON29 or CdTe-SON29 for different periods of time (ASON29: 5′-NH_2-AAA AAA AAA CCC AGC CTT CCA GCT CCT TG; SON29: 5′-NH_2-AAA AAA AAA CAA GGA GCT GGA AGG CTG GG). The scale bar in the micrograph corresponds to 10 μm (reprinted from ref. 153).

or carefully choosing thiols with suitable chemical structures, the family of low-dimensional CdTe nanomaterials also sees new members such as zero-dimensional CdTe nanocrystals potentially showing optical activity, CdTe nanowires and nanosheets formed upon self-assembly of zero-dimensional CdTe nanocrystals. Therefore, there are enough reasons to believe that the low-dimensional CdTe nanomaterials synthesized by the aqueous synthetic route will still be a hot subject in the coming years.

With respect to applications, CdTe nanocrystals and CdTe-based alloyed nanocrystals show a wide emission range covering especially the near-infrared region, which is not only interesting for photonics, optoelectronics, high-throughput immunoassays, but also for *in vivo* molecular imaging. Although the cytotoxicity of cadmium-containing materials is a huge hurdle towards bioapplications, it is not necessary to expect medicines out of CdTe nanocrystals. So far, the fluorescent II–VI semiconductor nanocrystals remain the most unique and irreplaceable model materials for extracting knowledge to meet the forthcoming nanomedicine in the near future.

Acknowledgements

The current investigations are jointly supported by National Basic Research Program of China (2011CB935800) and NSFC projects (81090271, 21003135, 20820102035), CAS project (KJCX2-YW-M15), 863 project (2010AA06Z302), and Croucher Foundation project (9220054).

References

1 A. Henglein, *Chem. Rev.*, 1989, **89**, 1861–1873.
2 U. Resch, H. Weller and A. Henglein, *Langmuir*, 1989, **5**, 1015–1020.
3 C. B. Murray, D. J. Norris and M. G. Bawendi, *J. Am. Chem. Soc.*, 1993, **115**, 8706–8715.
4 A. P. Alivisatos, *J. Phys. Chem.*, 1996, **100**, 13226–13239.
5 C. R. Kagan, C. B. Murray and M. G. Bawendi, *Phys. Rev. B: Condens. Matter*, 1996, **54**, 8633–8643.
6 M. Bruchez, M. Moronne, P. Gin, S. Weiss and A. P. Alivisatos, *Science*, 1998, **281**, 2013–2016.
7 W. C. W. Chan and S. M. Nie, *Science*, 1998, **281**, 2016–2018.
8 M. Nirmal and L. Brus, *Acc. Chem. Res.*, 1999, **32**, 407–414.
9 I. L. Medintz, H. T. Uyeda, E. R. Goldman and H. Mattoussi, *Nat. Mater.*, 2005, **4**, 435–446.
10 X. Michalet, F. F. Pinaud, L. A. Bentolila, J. M. Tsay, S. Doose, J. J. Li, G. Sundaresan, A. M. Wu, S. S. Gambhir and S. Weiss, *Science*, 2005, **307**, 538–544.
11 Z. A. Peng and X. G. Peng, *J. Am. Chem. Soc.*, 2001, **123**, 183–184.
12 L. H. Qu, Z. A. Peng and X. G. Peng, *Nano Lett.*, 2001, **1**, 333–337.
13 P. Reiss, M. Protiere and L. Li, *Small*, 2009, **5**, 154–168.
14 N. Gaponik, S. G. Hickey, D. Dorfs, A. L. Rogach and A. Eychmüller, *Small*, 2010, **6**, 1364–1378.
15 M. D. Regulacio and M. Y. Han, *Acc. Chem. Res.*, 2010, **43**, 621–630.
16 A. Henglein, *Ber. Bunsen-Ges. Phys. Chem.*, 1982, **86**, 301–305.
17 T. Vossmeyer, G. Reck, L. Katsikas, E. T. K. Haupt, B. Schulz and H. Weller, *Inorg. Chem.*, 1995, **34**, 4926–4929.
18 Y. Nosaka, H. Shigeno and T. Ikeuchi, *J. Phys. Chem.*, 1995, **99**, 8317–8322.
19 A. L. Rogach, A. Kornowski, M. Gao, A. Eychmüller and H. Weller, *J. Phys. Chem. B*, 1999, **103**, 3065–3069.
20 T. Rajh, O. I. Micic and A. J. Nozik, *J. Phys. Chem.*, 1993, **97**, 11999–12003.
21 A. L. Rogach, L. Katsikas, A. Kornowski, D. Su, A. Eychmüller and H. Weller, *Ber. Bunsen-Ges. Phys. Chem.*, 1997, **101**, 1668–1670.
22 A. L. Rogach, L. Katsikas, A. Kornowski, D. S. Su, A. Eychmüller and H. Weller, *Ber. Bunsen-Ges. Phys. Chem.*, 1996, **100**, 1772–1778.
23 M. Y. Gao, S. Kirstein, H. Möhwald, A. L. Rogach, A. Kornowski, A. Eychmüller and H. Weller, *J. Phys. Chem. B*, 1998, **102**, 8360–8363.
24 C. B. Murray, C. R. Kagan and M. G. Bawendi, *Annu. Rev. Mater. Sci.*, 2000, **30**, 545–610.
25 A. L. Rogach, T. Franzl, T. A. Klar, J. Feldmann, N. Gaponik, V. Lesnyak, A. Shavel, A. Eychmüller, Y. P. Rakovich and J. F. Donegan, *J. Phys. Chem. C*, 2007, **111**, 14628–14637.
26 N. Gaponik, D. V. Talapin, A. L. Rogach, K. Hoppe, E. V. Shevchenko, A. Kornowski, A. Eychmüller and H. Weller, *J. Phys. Chem. B*, 2002, **106**, 7177–7185.
27 A. L. Rogach, N. Gaponik, J. M. Lupton, C. Bertoni, D. E. Gallardo, S. Dunn, N. L. Pira, M. Paderi, P. Repetto, S. G. Romanov, C. O'Dwyer, C. M. S. Torres and A. Eychmüller, *Angew. Chem., Int. Ed.*, 2008, **47**, 6538–6549.v
28 N. Gaponik and A. L. Rogach, *Phys. Chem. Chem. Phys.*, 2010, **12**, 8685–8693.
29 K. T. Yong, I. Roy, W. C. Law and R. Hu, *Chem. Commun.*, 2010, **46**, 7136–7138.
30 A. Zintchenko, A. S. Susha, M. Concia, J. Feldmann, E. Wagner, A. L. Rogach and M. Ogris, *Mol. Ther.*, 2009, **17**, 1849–1856.

31 H. B. Bao, Y. J. Gong, Z. Li and M. Y. Gao, *Chem. Mater.*, 2004, **16**, 3853–3859.
32 D. E. Dunstan, A. Hagfeldt, M. Almgren, H. O. G. Siegbahn and E. Mukhtar, *J. Phys. Chem.*, 1990, **94**, 6797–6804.
33 S. R. Cordero, P. J. Carson, R. A. Estabrook, G. F. Strouse and S. K. Buratto, *J. Phys. Chem. B*, 2000, **104**, 12137–12142.
34 D. V. Talapin, A. L. Rogach, E. V. Shevchenko, A. Kornowski, M. Haase and H. Weller, *J. Am. Chem. Soc.*, 2002, **124**, 5782–5790.
35 H. Asami, Y. Abe, T. Ohtsu, I. Kamiya and M. Hara, *J. Phys. Chem. B*, 2003, **107**, 12566–12568.
36 A. Shavel, N. Gaponik and A. Eychmüller, *J. Phys. Chem. B*, 2004, **108**, 5905–5908.
37 M. Y. Gao, X. Zhang, B. Yang, F. Li and J. C. Shen, *Thin Solid Films*, 1996, **284–285**, 242–245.
38 I. G. Dance, M. L. Scudder and R. Secomb, *Inorg. Chem.*, 1983, **22**, 1794–1797.
39 H. J. Niu and M. Y. Gao, *Angew. Chem., Int. Ed.*, 2006, **45**, 6462–6466.
40 H. Zhang, Z. Zhou, B. Yang and M. Y. Gao, *J. Phys. Chem. B*, 2003, **107**, 8–13.
41 H. F. Qian, C. Q. Dong, J. F. Weng and J. C. Ren, *Small*, 2006, **2**, 747–751.
42 Y. G. Zheng, S. J. Gao and J. Y. Ying, *Adv. Mater.*, 2007, **19**, 376–380.
43 Y. F. Liu and J. S. Yu, *J. Colloid Interface Sci.*, 2010, **351**, 1–9.
44 W. W. Li, J. Liu, K. Sun, H. J. Dou and K. Tao, *J. Mater. Chem.*, 2010, **20**, 2133–2138.
45 Y. F. Kong, J. Chen, F. Gao, W. T. Li, X. Xu, O. Pandoli, H. Yang, J. J. Ji and D. X. Cui, *Small*, 2010, **6**, 2367–2373.
46 L. Zou, Z. Gu, N. Zhang, Y. Zhang, Z. Fang, W. Zhu and X. Zhong, *J. Mater. Chem.*, 2008, **18**, 2807–2815.
47 A. Priyam, S. Ghosh, S. C. Bhattachcarya and A. Saha, *J. Colloid Interface Sci.*, 2009, **333**, 195–201.
48 H. Zhang, D. Wang, B. Yang and H. Möhwald, *J. Am. Chem. Soc.*, 2006, **128**, 10171–10180.
49 Z. Y. Tang, N. A. Kotov and M. Giersig, *Science*, 2002, **297**, 237–240.
50 S. Srivastava, A. Santos, K. Critchley, K. S. Kim, P. Podsiadlo, K. Sun, J. Lee, C. L. Xu, G. D. Lilly, S. C. Glotzer and N. A. Kotov, *Science*, 2010, **327**, 1355–1359.
51 H. Peng, L. J. Zhang, C. Soeller and J. Travas-Sejdic, *J. Lumin.*, 2007, **127**, 721–726.
52 Z. Y. Gu, L. Zou, Z. Fang, W. H. Zhu and X. H. Zhong, *Nanotechnology*, 2008, **19**, 135604.
53 Y. F. Liu and J. S. Yu, *J. Colloid Interface Sci.*, 2009, **333**, 690–698.
54 Y. He, H. T. Lu, L. M. Sai, W. Y. Lai, Q. L. Fan, L. H. Wang and W. Huang, *J. Phys. Chem. B*, 2006, **110**, 13370–13374.
55 C. Wang, H. Zhang, J. Zhang, M. Li, H. Sun and B. Yang, *J. Phys. Chem. C*, 2007, **111**, 2465–2469.
56 J. J. Li, Y. A. Wang, W. Guo, J. C. Keay, T. D. Mishima, M. B. Johnson and X. Peng, *J. Am. Chem. Soc.*, 2003, **125**, 12567–12575.
57 Q. H. Zeng, X. G. Kong, Y. J. Sun, Y. L. Zhang, L. P. Tu, J. L. Zhao and H. Zhang, *J. Phys. Chem. C*, 2008, **112**, 8587–8593.
58 D. Zhao, Z. K. He, W. H. Chan and M. M. F. Choi, *J. Phys. Chem. C*, 2009, **113**, 1293–1300.
59 Y. Zhang, Y. Li and X. P. Yan, *Small*, 2008, **5**, 185–189.
60 W. C. Law, K. T. Yong, I. Roy, H. Ding, R. Hu, W. W. Zhao and P. N. Prasad, *Small*, 2009, **5**, 1302–1310.
61 M. Green, P. Williamson, M. Samalova, J. Davis, S. Brovelli, P. Dobson and F. Cacialli, *J. Mater. Chem.*, 2009, **19**, 8341–8346.
62 Y. He, H. T. Lu, L. M. Sai, Y. Y. Su, M. Hu, C. H. Fan, W. Huang and L. H. Wang, *Adv. Mater.*, 2008, **20**, 3416–3421.
63 Z. Y. Tang, Y. Wang, S. Shanbhag and N. A. Kotov, *J. Am. Chem. Soc.*, 2006, **128**, 7036–7042.
64 N. Piven, A. S. Susha, M. Doeblinger and A. L. Rogach, *J. Phys. Chem. C*, 2008, **112**, 15253–15259.
65 H. Qian, C. Dong, J. Peng, X. Qiu, Y. Xu and J. Ren, *J. Phys. Chem. C*, 2007, **111**, 16852–16857.
66 H. Z. Sun, H. Zhang, J. Ju, J. H. Zhang, G. Qian, C. L. Wang, B. Yang and Z. Y. Wang, *Chem. Mater.*, 2008, **20**, 6764–6769.
67 V. Lesnyak, A. Lutich, N. Gaponik, M. Grabolle, A. Plotnikov, U. Resch-Genger and A. Eychmüller, *J. Mater. Chem.*, 2009, **19**, 9147–9152.
68 Y. L. Zhou, M. Yang, K. Sun, Z. Y. Tang and N. A. Kotov, *J. Am. Chem. Soc.*, 2010, **132**, 6006–6013.
69 H. Zhang, L. P. Wang, H. M. Xiong, L. H. Hu, B. Yang and W. Li, *Adv. Mater.*, 2003, **15**, 1712–1715.
70 Y. He, L. M. Sai, H. T. Lu, M. Hu, W. Y. Lai, Q. L. Fan, L. H. Wang and W. Huang, *Chem. Mater.*, 2007, **19**, 359–365.
71 Y. He, H. T. Lu, L. M. Sai, W. Y. Lai, Q. L. Fan, L. H. Wang and W. Huang, *J. Phys. Chem. B*, 2006, **110**, 13352–13356.
72 L. Li, H. F. Qian and J. C. Ren, *Chem. Commun.*, 2005, 528–530.
73 S. Baral, A. Fojtik, H. Weller and A. Henglein, *J. Am. Chem. Soc.*, 1986, **108**, 375–378.
74 S. K. Poznyak, N. P. Osipovich, A. Shavel, D. V. Talapin, M. Y. Gao, A. Eychmüller and N. Gaponik, *J. Phys. Chem. B*, 2005, **109**, 1094–1100.
75 X. Gao and S. Nie, *Anal. Chem.*, 2004, **76**, 2406–2410.
76 M. Y. Han, X. H. Gao, J. Z. Su and S. Nie, *Nat. Biotechnol.*, 2001, **19**, 631–635.
77 M. A. Correa-Duarte, M. Giersig and L. M. Liz-Marzán, *Chem. Phys. Lett.*, 1998, **286**, 497–501.
78 S. Y. Chang, L. Liu and S. A. Asher, *J. Am. Chem. Soc.*, 1994, **116**, 6739–6744.
79 A. L. Rogach, D. Nagesha, J. W. Ostrander, M. Giersig and N. A. Kotov, *Chem. Mater.*, 2000, **12**, 2676–2685.
80 D. Gerion, F. Pinaud, S. C. Williams, W. J. Parak, D. Zanchet, S. Weiss and A. P. Alivisatos, *J. Phys. Chem. B*, 2001, **105**, 8861–8871.
81 S. Santra, P. Zhang, K. Wang, R. Tapec and W. Tan, *Anal. Chem.*, 2001, **73**, 4988–4993.
82 A. Schroedter, H. Weller, R. Eritja, W. E. Ford and J. M. Wessels, *Nano Lett.*, 2002, **2**, 1363–1367.
83 Y. Chan, J. P. Zimmer, M. Stroh, J. S. Steckel, R. K. Jain and M. G. Bawendi, *Adv. Mater.*, 2004, **16**, 2092–2097.
84 T. Nann and P. Mulvaney, *Angew. Chem.,Int. Ed.*, 2004, **43**, 5393–5396.
85 T. Mokari, H. Sertchook, A. Aharoni, Y. Ebenstein, D. Avnir and U. Banin, *Chem. Mater.*, 2005, **17**, 258–263.
86 S. T. Selvan, C. L. Li, M. Ando and N. Murase, *Chem. Lett.*, 2004, **33**, 434–435.
87 Y. H. Yang and M. Y. Gao, *Adv. Mater.*, 2005, **17**, 2354–2357.
88 Y. H. Yang, L. H. Jing, X. L. Yu, D. D. Yan and M. Y. Gao, *Chem. Mater.*, 2007, **19**, 4123–4128.
89 L. H. Jing, C. H. Yang, R. R. Qiao, M. Niu, M. H. Du, D. Y. Wang and M. Y. Gao, *Chem. Mater.*, 2010, **22**, 420–427.
90 K. Osseo-Asare and F. J. Arriagada, *Colloids Surf.*, 1990, **50**, 321–339.
91 C. L. Chang and H. S. Fogler, *Langmuir*, 1997, **13**, 3295–3307.
92 F. J. Arriagada and K. Osseo-Asare, *J. Colloid Interface Sci.*, 1999, **211**, 210–220.
93 N. Tomczak, D. Janczewski, M. Y. Han and G. J. Vancso, *Prog. Polym. Sci.*, 2009, **34**, 393–430.
94 M. Kuang, D. Y. Wang, H. B. Bao, M. Y. Gao, H. Möhwald and M. Jiang, *Adv. Mater.*, 2005, **17**, 267–270.
95 Y. J. Gong, M. Y. Gao, D. Y. Wang and H. Möhwald, *Chem. Mater.*, 2005, **17**, 2648–2653.
96 Y. H. Yang, Z. K. Wen, Y. P. Dong and M. Y. Gao, *Small*, 2006, **2**, 898–901.
97 Y. H. Yang, C. F. Tu and M. Y. Gao, *J. Mater. Chem.*, 2007, **17**, 2930–2935.
98 F. Bian, J. Cai, X. Liu, M. Gao, C. Zhang, S. J. J. Ma and Y. Liu, *Acta Sci. Natur. Univ. Jilinensis*, 1994, **4**, 115–117.
99 M. Y. Gao, Y. Yang, B. Yang, J. C. Shen and X. C. Ai, *J. Chem. Soc., Faraday Trans.*, 1995, **91**, 4121–4125.
100 M. Y. Gao, M. L. Gao, X. Zhang, Y. Yang, B. Yang and J. C. Shen, *J. Chem. Soc., Chem. Commun.*, 1994, 2777–2778.

101 M. Y. Gao, Y. Yang, B. Yang, F. L. Bian and J. C. Shen, *J. Chem. Soc., Chem. Commun*., 1994, 2779–2780.
102 M. Y. Gao, Y. Yang, B. Yang and J. Shen, *Proceeding of China–Japan Bilateral Symposium on Polymer Materials Science*, Huangshan, China, 1995.
103 C. F. Tu, Y. H. Yang and M. Y. Gao, *Nanotechnology*, 2008, **19**, 105601.
104 H. Zhang, Z. Cui, Y. Wang, K. Zhang, X. Ji, C. Lü, B. Yang and M. Gao, *Adv. Mater*., 2003, **15**, 777–780.
105 H. Li, P. Li, Y. Yang, W. Qi, H. Sun and L. Wu, *Macromol. Rapid Commun*., 2008, **29**, 431–436.
106 Z. Y. Tang, Z. Zhang, Y. Wang, S. C. Glotzer and N. A. Kotov, *Science*, 2006, **314**, 274–278.
107 N. Gaponik, A. Wolf, R. Marx, V. Lesnyak, K. Schilling and A. Eychmüller, *Adv. Mater*., 2008, **20**, 4257–4262.
108 H. J. Niu, L. W. Zhang, M. Y. Gao and Y. M. Chen, *Langmuir*, 2005, **21**, 4205–4210.
109 J. Li, X. Hong, D. Li, K. Zhao, L. Wang, H. Z. Wang, Z. L. Du, J. H. Li, Y. B. Bai and T. J. Li, *Chem. Commun*., 2004, 1740–1741.
110 L. Manna, D. J. Milliron, A. Meisel, E. C. Scher and A. P. Alivisatos, *Nat. Mater*., 2003, **2**, 382–385.
111 W. W. Yu, Y. A. Wang and X. Peng, *Chem. Mater*., 2003, **15**, 4300–4308.
112 H. Zhang, D. Wang and H. Möhwald, *Angew. Chem., Int. Ed*., 2006, **45**, 6244–6244.
113 F. Z. Khan and P. O'Brien, *Polyhedron*, 1991, **10**, 325–332.
114 J. C. Bayon, M. C. Brianso, J. L. Brianso and P. G. Duarte, *Inorg. Chem*., 1979, **18**, 3478–3482.
115 P. Yang, M. Ando and N. Murase, *Adv. Mater*., 2009, **21**, 4016–4019.
116 H. Chen, V. Lesnyak, N. C. Bigall, N. Gaponik and A. Eychmüller, *Chem. Mater*., 2010, **22**, 2309–2314.
117 A. L. Rogach, T. A. Klar, J. M. Lupton, A. Meijerink and J. Feldmann, *J. Mater. Chem*., 2009, **19**, 1208–1221.
118 H. Mattoussi, L. H. Radzilowski, B. O. Dabbousi, E. L. Thomas, M. G. Bawendi and M. F. Rubner, *J. Appl. Phys*., 1998, **83**, 7965–7974.
119 B. O. Dabbousi, M. G. Bawendi, O. Onitsuka and M. F. Rubner, *Appl. Phys. Lett*., 1995, **66**, 1316–1318.
120 M. C. Schlamp, X. G. Peng and A. P. Alivisatos, *J. Appl. Phys*., 1997, **82**, 5837–5842.
121 B. O. Dabbousi, J. RodriguezViejo, F. V. Mikulec, J. R. Heine, H. Mattoussi, R. Ober, K. F. Jensen and M. G. Bawendi, *J. Phys. Chem. B*, 1997, **101**, 9463–9475.
122 X. G. Peng, M. C. Schlamp, A. V. Kadavanich and A. P. Alivisatos, *J. Am. Chem. Soc*., 1997, **119**, 7019–7029.
123 M. A. Hines and P. Guyot-Sionnest, *J. Phys. Chem*., 1996, **100**, 468–471.
124 A. Mews, A. Eychmüller, M. Giersig, D. Schooss and H. Weller, *J. Phys. Chem*., 1994, **98**, 934–941.
125 A. L. Efros, M. Rosen, M. Kuno, M. Nirmal, D. J. Norris and M. Bawendi, *Phys. Rev. B: Condens. Matter*, 1996, **54**, 4843–4856.
126 M. Nirmal, D. J. Norris, M. Kuno, M. G. Bawendi, A. L. Efros and M. Rosen, *Phys. Rev. Lett*., 1995, **75**, 3728–3731.
127 G. Decher, *Science*, 1997, **277**, 1232–1237.
128 N. Gaponik, *J. Mater. Chem*., 2010, **20**, 5174–5181.
129 A. Shavel, N. Gaponik and A. Eychmüller, *Eur. J. Inorg. Chem*., 2005, **18**, 3613–3623.
130 S. Srivastava and N. A. Kotov, *Acc. Chem. Res*., 2008, **41**, 1831–1841.
131 Y. Lvov, G. Decher and H. Möhwald, *Langmuir*, 1993, **9**, 481–486.
132 Y. Sun, E. Hao, X. Zhang, B. Yang, M. Gao and J. Shen, *Chem. Commun*., 1996, 2381–2382.
133 M. Y. Gao, X. Zhang, B. Yang and J. Shen, *J. Chem. Soc., Chem. Commun*., 1994, 2229–2230.
134 N. A. Kotov, F. C. Meldrum, J. H. Fendler, E. Tombacz and I. Dekany, *Langmuir*, 1994, **10**, 3797–3804.
135 N. A. Kotov, F. C. Meldrum, C. Wu and J. H. Fendler, *J. Phys. Chem*., 1994, **98**, 2735–2738.
136 N. A. Kotov, I. Dekany and J. H. Fendler, *J. Phys. Chem*., 1995, **99**, 13065–13069.
137 M. Y. Gao, B. Richter and S. Kirstein, *Adv. Mater*., 1997, **9**, 802–805.
138 M. Y. Gao, B. Richter, S. Kirstein and H. Möhwald, *J. Phys. Chem. B*, 1998, **102**, 4096–4103.
139 M. Y. Gao, S. Kirstein, A. L. Rogach, H. Weller and H. Möhwald, in *Advances in Science and Technology 27: Innovative Light Emitting Materials*, ed. P. Vincenzini and G. C. Righini, Techna Srl., Italy, 1999, pp. 347–358.
140 M. Y. Gao, B. Richter and S. Kirstein, *Synth. Met*., 1999, **102**, 1213–1214.
141 M. Y. Gao, C. Lesser, S. Kirstein, H. Möhwald, A. L. Rogach and H. Weller, *J. Appl. Phys*., 2000, **87**, 2297–2302.
142 J. Q. Sun, M. Y. Gao and J. Feldmann, *J. Nanosci. Nanotechnol*., 2001, **1**, 133–136.
143 M. Y. Gao, B. Richter and S. Kirstein, *Adv. Mater*., 1997, **9**, 802–805.
144 C. Lesser, M. Y. Gao and S. Kirstein, *Mater. Sci. Eng., C*, 1999, **8–9**, 159–162.
145 C. Bertoni, D. Gallardo, S. Dunn, N. Gaponik and A. Eychmüller, *Appl. Phys. Lett*., 2007, **90**, 034107.
146 J. S. Bendall, M. Paderi, F. Ghigliotti, N. L. Pira, V. Lambertini, V. Lesnyak, N. Gaponik, G. Visimberga, A. Eychmüller, C. M. S. Torres, M. E. Welland, C. Gieck and L. Marchese, *Adv. Funct. Mater*., 2010, **20**, 3298–3302.
147 M. Y. Gao, J. Q. Sun, E. Dulkeith, N. Gaponik, U. Lemmer and J. Feldmann, *Langmuir*, 2002, **18**, 4098–4102.
148 L. X. Shi, J. Q. Sun, J. Q. Liu, J. C. Shen and M. Y. Gao, *Chem. Lett*., 2002, 1168–1169.
149 J. Q. Sun, M. Y. Gao, M. Zhu, J. Feldmann and H. Möhwald, *J. Mater. Chem*., 2002, **12**, 1775–1778.
150 S. P. Wang, N. Mamedova, N. A. Kotov, W. Chen and J. Studer, *Nano Lett*., 2002, **2**, 817–822.
151 Y. Zhang, L. Mi, J. Y. Chen and P. N. Wang, *Biomed. Mater*., 2009, **4**, 012001.
152 F. Q. Hu, Y. L. Ran, Z. A. Zhou and M. Y. Gao, *Nanotechnology*, 2006, **17**, 2972–2977.
153 Y. Li, X. Duan, L. Jing, C. Yang, R. Qiao and M. Gao, *Biomaterials*, 2011, **32**, 1923–1931.
154 B. Dubertret, P. Skourides, D. J. Norris, V. Noireaux, A. H. Brivanlou and A. Libchaber, *Science*, 2002, **298**, 1759–1762.
155 M. E. Åkerman, W. C. W. Chan, P. Laakkonen, S. N. Bhatia and E. Ruoslahti, *Proc. Natl. Acad. Sci. U. S. A*., 2002, **99**, 12617–12621.
156 B. Ballou, B. C. Lagerholm, L. A. Ernst, M. P. Bruchez and A. S. Waggoner, *Bioconjugate Chem*., 2004, **15**, 79–86.
157 M. Zheng, F. Davidson and X. Huang, *J. Am. Chem. Soc*., 2003, **125**, 7790–7791.
158 M. Zheng, Z. Li and X. Huang, *Langmuir*, 2004, **20**, 4226–4235.
159 D. Gerion, W. J. Parak, S. C. Williams, D. Zanchet, C. M. Micheel and A. P. Alivisatos, *J. Am. Chem. Soc*., 2002, **124**, 7070–7074.
160 E. L. Bentzen, I. D. Tomlinson, J. Mason, P. Gresch, M. R. Warnement, D. Wright, E. Sanders-Bush, R. Blakely and S. J. Rosenthal, *Bioconjugate Chem*., 2005, **16**, 1488–1494.
161 A. A. Chen, A. M. Derfus, S. R. Khetani and S. N. Bhatia, *Nucleic Acids Res*., 2005, **33**, e8.
162 C. Srinivasan, J. Lee, F. Papadimitrakopoulos, L. K. Silbart, M. H. Zhao and D. J. Burgess, *Mol. Ther*., 2006, **14**, 192–201.
163 A. M. Derfus, A. A. Chen, D. H. Min, E. Ruoslahti and S. N. Bhatia, *Bioconjugate Chem*., 2007, **18**, 1391–1396.
164 W. B. Tan, S. Jiang and Y. Zhang, *Biomaterials*, 2007, **28**, 1565–1571.
165 D. Li, G. P. Li, W. W. Guo, P. C. Li, E. K. Wang and J. Wang, *Biomaterials*, 2008, **29**, 2776–2782.
166 L. F. Qi and X. H. Gao, *ACS Nano*, 2008, **2**, 1403–1410.
167 C. Walther, K. Meyer, R. Rennert and I. Neundorf, *Bioconjugate Chem*., 2008, **19**, 2346–2356.
168 M. V. Yezhelyev, L. F. Qi, R. M. O'Regan, S. Nie and X. H. Gao, *J. Am. Chem. Soc*., 2008, **130**, 9006–9012.
169 J. J. Jung, A. Solanki, K. A. Memoli, K. Kamei, H. Kim, M. A. Drahl, L. J. Williams, H. R. Tseng and K. Lee, *Angew. Chem., Int. Ed*., 2010, **49**, 5708–107.

170 H. Lee, I. K. Kim and T. G. Park, *Bioconjugate Chem.*, 2010, **21**, 289–295.
171 Y. P. Ho, H. H. Chen, K. W. Leong and T. H. Wang, *J. Controlled Release*, 2006, **116**, 83–89.
172 N. Q. Jia, Q. Lian, H. B. Shen, C. Wang, X. Y. Li and Z. N. Yang, *Nano Lett.*, 2007, **7**, 2976–2980.
173 M. A. Mintzer and E. E. Simanek, *Chem. Rev.*, 2009, **109**, 259–302.
174 T. Gratieri, U. F. Schaefer, L. H. Jing, M. Y. Gao, K. H. Kostka, R. F. V. Lopez and M. Schneider, *J. Biomed. Nanotechnol.*, 2010, **6**, 586–595.
175 J. Lovric, H. S. Bazzi, Y. Cuie, G. R. A. Fortin, F. M. Winnik and D. Maysinger, *J. Mol. Med.*, 2005, **83**, 377–385.
176 S. J. Cho, D. Maysinger, M. Jain, B. Roder, S. Hackbarth and F. M. Winnik, *Langmuir*, 2007, **23**, 1974–1980.